

AD 654129



AD

TECHNICAL REPORT ECOM-02192 2

RELATIONSHIPS BETWEEN TROPICAL PRECIPITATION AND KINEMATIC CLOUD MODELS

ANNUAL REPORT NO. 1

By

GEIRMUNDUR ARNASON

R. S. GREENFIELD

Distribution of this document
is unlimited

JUNE 1967

BEST AVAILABLE COPY

ECOM

UNITED STATES ARMY ELECTRONICS COMMAND · FORT MONMOUTH, N.J.

CONTRACT NO. DA 28-043-AMC-02192(E)

THE TRAVELERS RESEARCH CENTER, INC.

250 CONSTITUTION PLAZA HARTFORD, CONNECTICUT 06103

2004083/027

RELATIONSHIPS BETWEEN TROPICAL PRECIPITATION
AND KINEMATIC CLOUD MODELS

ANNUAL REPORT NO. 1

1 NOVEMBER 1966 - 30 APRIL 1967

CONTRACT NO. DA 28-043-AMC-02192(E)

7482-257

Prepared by

G. Árnason and R. S. Greenfield

THE TRAVELERS RESEARCH CENTER, INC.

250 Constitution Plaza

Hartford, Connecticut

06103

for

ATMOSPHERIC SCIENCES LABORATORY

U.S. ARMY ELECTRONICS COMMAND, FORT MONMOUTH, N.J.

DISTRIBUTION OF THIS DOCUMENT IS UNLIMITED

75018804005



NOTICES

Disclaimers

The findings in this report are not to be construed as an official Department of the Army position, unless so designated by other authorized documents.

The citation of trade names and names of manufacturers in this report is not to be construed as official Government indorsement or approval of commercial products or services referenced herein.

Disposition

Destroy this report when it is no longer needed. Do not return it to the originator.

ABSTRACT

The mathematical formulation and associated finite-difference approximations for the numerical model of a precipitating roll cloud are summarized. With that background, the computer program used to perform the computations in experiments simulating moist convection is described in detail.

The program description includes discussion of the input requirements, the internal operations, and the output. The newly developed recovery feature of the program is explained. All options, presently available in the program, are described. The detailed description of the computer program is contained in individual flow diagrams of the main program and the 16 sub-routines.

In the concluding remarks, the present status of the computer program is given. Finally, the anticipated future plans for the program are outlined.

ACKNOWLEDGEMENT

The authors gratefully acknowledge the tireless efforts of Miss Peggy Atticks in her skillful typing of this manuscript, including her devotion to the task of transforming nearly unintelligible flow charts into well coordinated flow diagrams.

TABLE OF CONTENTS

<u>Section</u>	<u>Title</u>	<u>Page</u>
1.0	INTRODUCTION	1
2.0	SUMMARY OF MATHEMATICAL FORMULATION OF THE MODEL	3
2.1	The Perturbation-Basic-State Approach	3
2.2	The Equations Governing the Dynamics and Thermodynamics of the Perturbation-Basic-State System	4
2.3	Equations Governing the Macrophysics of Water Substance	7
2.4	Boundary and Initial Conditions	10
2.5	The Diagnostic Pressure Equation	11
3.0	SUMMARY OF FINITE-DIFFERENCE APPROXIMATIONS	13
3.1	Finite-Difference Equations Used for the Interior Points	13
3.1.1	The centered-difference approximations	13
3.1.2	The Lax-Wendroff scheme applied to the equations for heat and water substance	15
3.2	Boundary Conditions	17
3.3	Initial Time Step Approximation	19
4.0	THE INITIAL DATA	21
5.0	PROGRAM DESCRIPTION	24
5.1	Input	24
5.1.1	Control variables	24
5.1.2	Program constants	25
5.1.3	Input format	25
5.2	Internal Operations	26
5.2.1	Subroutine operations	27
5.2.2	General Flow	28

TABLE OF CONTENTS (Continued)

<u>Section</u>	<u>Title</u>	<u>Page</u>
5.3	Output	29
5.3.1	Form	29
5.3.2	Controls and options available	30
5.3.3	Anticipated changes	30
5.4	Recovery	31
5.4.1	Method	32
5.4.2	Available options and associated input controls	32
6.0	CONCLUSIONS	34
6.1	Present Status	34
6.2	Future Plans	34
7.0	LITERATURE CITED	36

APPENDIX A - List of Symbols

APPENDIX B - Flow Diagrams

LIST OF ILLUSTRATIONS

<u>Figure</u>	<u>Title</u>	<u>Page</u>
1	Convective cell: geometry and boundary conditions	5
2	Initial potential temperature perturbation in °C	23
B-1	MAIN - Directs general flow of computations	B-3
B-2	PRTIN - Prints "dry" input	B-7
B-3	MØISIN - Reads and prints "moist" input; computes and prints initial q_s and q fields	B-8
B-4	RELAX1 - Performs relaxation of ψ -field; prints convergence information	B-10
B-5	RELAX2 - Performs relaxation of p -field; prints convergence information	B-12
B-6	HYPRES - Computes hydrostatic pressure (P_2)	B-17
B-7	CSBR - Computes source function for θ -prediction	B-18
B-8	PRDCTM - Computes source functions for, and controls prediction of q_p , q_s , and q	B-19
B-9	PREDIN - Predicts values of q_p , q_s , and q for interior points	B-24
B-10	PREDUL - Predicts upper and lower boundary values of q_p , q_s , and q	B-25
B-11	PREDLR - Predicts lateral boundary values of q_p , q_s , and q	B-26
B-12	EXCNG - Selectively controls flow of arrays to and from auxiliary storage	B-27
B-13	SMØØTH - Transfers fields from dummy array (DUMA) to proper array	B-28
B-14	DUMP - Prints source functions for θ and q_p	B-29
B-15	SUMPK - Computes and prints space averaged potential and kinetic energies and their difference	B-30
B-16	SUMTB - Computes and prints space averaged potential temperature	B-33
B-17	PRINTOUT - Prints the θ , ψ , ζ , p , P_2 , q_{cl} , q_p , q_s , and q fields	B-34

LIST OF TABLES

<u>Number</u>	<u>Title</u>	<u>Page</u>
1	Basic-state distribution with height of potential temperature, temperature, density, pressure, saturation vapor pressure, and relative humidity	22
2	Input of control variables to the program	24
3	Input of program constants to the program	25
4	Input card format	26
5	Purpose of program subroutines	27
B-1	Flow diagram symbols	B-2

1.0 INTRODUCTION

Under two consecutive contracts with the U.S. Army Electronics Command, work has progressed for three years toward the development of a mathematical model which simulates shallow, moist convection culminating in a precipitating cloud. The theoretical formulation of the model was presented at the outset of the model development [1]. Included in that report is an extensive discussion of the literature relating to convection. Subsequent reports [2, 3, 4] have described the successive developmental stages leading to the present model of a precipitating roll cloud.

The simulation experiments are carried out by numerically integrating the model equations with suitable boundary and initial conditions. The integrations are performed by an electronic digital computer. At present, the computer being used is the UNIVAC 1108 system.

Because the model has been developed to the point that meaningful simulation experiments can be performed, it is felt that a summary of the model, and a detailed description of the associated computer program is desirable. This report is primarily a description of the rather complicated computer program which controls numerical computations involved in the simulation experiments.

Section 2.0 of this report summarizes the mathematical formulation of the model. The summary is composed of five subsections: 2.1 deals with the perturbation-basic-state approach; 2.2 covers the dynamics and thermodynamics of the mathematical system; 2.3 reviews the macrophysics associated with water substance (vapor, cloud, and precipitation); 2.4 summarizes the boundary and initial conditions; and 2.5 discusses the diagnostic equation used to determine the dynamic pressure.

Section 3.0 presents a summary of the finite-difference approximations used to perform the numerical computations. The finite-difference approximations are considered separately as they apply to the interior points, to the boundary points, and to the initial time step. The initial data is reviewed in Section 4.0.

Section 5.0 contains a detailed program description. This description is presented in four broad categories. These are input required by the program, internal operations controlled by the program, output, and the recovery feature of the program.

Section 6.0 contains concluding remarks about the program with respect to the present status and future plans in the utilization of the model.

Appendix A contains a description of the symbols and Appendix B contains the detailed flow diagrams of the entire program.

2.0 SUMMARY OF MATHEMATICAL FORMULATION OF THE MODEL

The theoretical development of the model was treated in detail in an earlier report [1]. This report will merely summarize the mathematical formulation to provide a frame of reference for the program.

2.1 The Perturbation-Basic-State Approach

The shallow convection, which ultimately leads to a precipitating roll cloud, is initiated by introducing a buoyant bubble into a model atmosphere initially at rest and horizontally uniform. The initial state of the model is considered to be composed of two parts:

- a) a basic state, and
- b) superimposed perturbations.

The undisturbed model atmosphere is the basic state. Therefore, the physical variables associated with the basic state are functions of the vertical coordinate only. These are potential temperature θ_0 , density ρ_0 , pressure p_0 , saturation vapor pressure e_{s0} , and relative humidity r_0 .

The initial superimposed perturbation consists of the buoyant bubble. All departures from the basic state become a part of the perturbation fields. Therefore, the physical variables characterizing the perturbations are functions of the spatial and temporal coordinates.

The perturbation-basic-state approach provides a natural scaling of the variables which must be predicted by the computer. It is well known that scaling the variables in a multi-iterative problem is quite useful in reducing the possibility that round-off error will corrupt the solution.

2.2 The Equations Governing the Dynamics and Thermodynamics of the Perturbation-Basic-State System

The convective cell is bounded vertically by two rigid horizontal planes a distance H (3 km) apart. Laterally, on two opposing sides, the model is bounded by two rigid vertical planes a distance $2L$ (6 km) apart and of infinite horizontal extent. Midway between the vertical planes on the lower of the two horizontal planes, the origin of a Cartesian coordinate system is established with the x -axis normal to the vertical planes and the z -axis normal to the horizontal planes, as shown in Fig. 1. All physical variables are assumed always independent of y , and symmetry about the plane $x = 0$ is imposed. The symmetry is imposed through an initially symmetric temperature perturbation. Thereafter, the boundary conditions and governing physical laws require the dependent variables to be either even or odd functions with respect to x (symmetry condition). By virtue of the symmetry condition, the domain of solution of the numerical solution is $0 \leq x \leq L$, $0 \leq z \leq H$.

Over that domain, the dynamic equations for shallow convection are the continuity equation

$$\nabla \cdot \vec{v} = 0, \quad (2-1)$$

and the momentum equation

$$\frac{\partial}{\partial t} \vec{v} + \vec{v} \cdot \nabla \vec{v} + \frac{\rho}{\rho_0} g \vec{k} + \frac{1}{\rho_0} \nabla p = 0, \quad (2-2)$$

where \vec{v} is the wind with components u and w , ρ is the density, p is the pressure, and g is the acceleration of gravity. Subscript zero indicates the basic state, and perturbation quantities are without subscript. By taking the curl of Eq. (2-2), the vorticity equation

$$\frac{\partial \zeta}{\partial t} + \vec{v} \cdot \nabla \zeta + \frac{g}{\rho_0} \frac{\partial \rho}{\partial x} = 0, \quad (2-3)$$

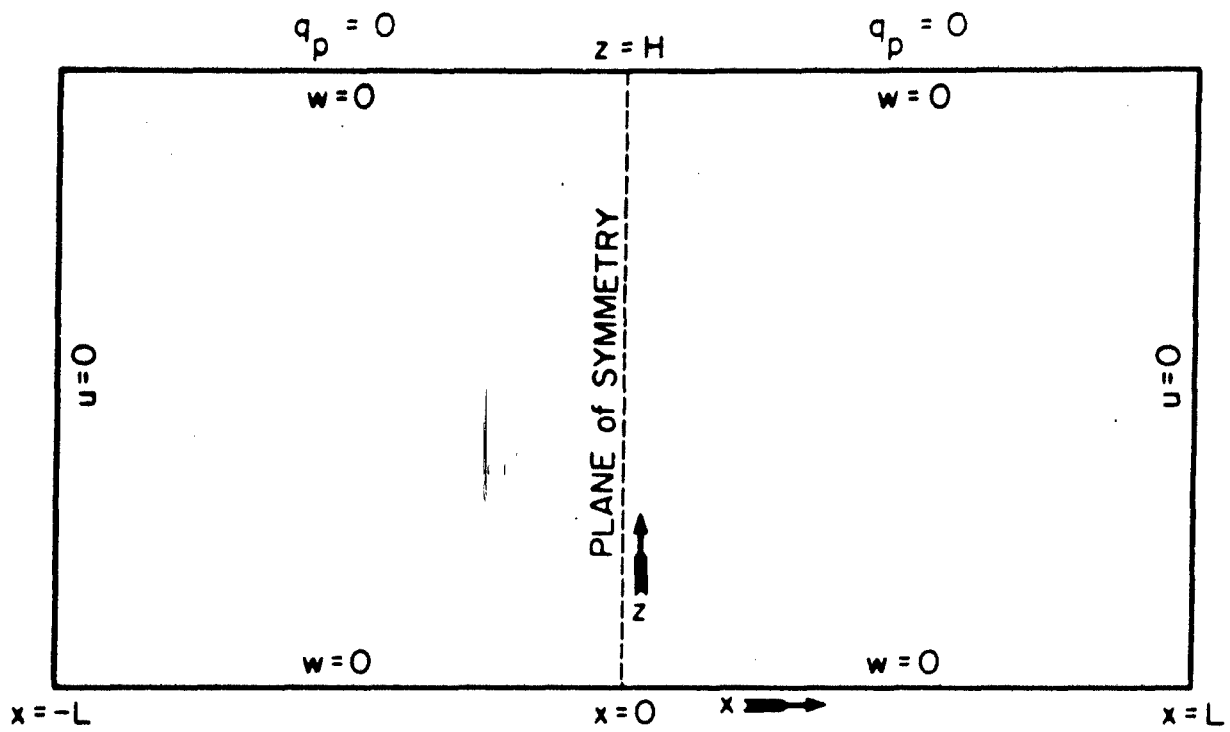


Fig. 1. Convective cell: geometry and boundary conditions.

is obtained, where ζ is the relative vorticity $(\partial w / \partial x) - (\partial u / \partial z)$. Introduction of the stream function ψ , defined by $\vec{v} = u\vec{i} + w\vec{k} = \mathbf{k} \times \nabla\psi$, so that

$$u = -\frac{\partial\psi}{\partial z}, \quad w = \frac{\partial\psi}{\partial x} \quad (2-4)$$

satisfies Eq. (2-1) without further restriction on the motion field. Moreover, the vorticity is given by

$$\zeta = \nabla^2\psi, \quad (2-5)$$

where $\nabla^2(\) \equiv \partial^2(\)/\partial x^2 + \partial^2(\)/\partial z^2$.

The stream function may be predicted by means of Eqs. (2-3), (2-4), and (2-5), provided the density is known. It can be shown (see [1], [3]), that for shallow, moist convection,

$$\frac{\rho}{\rho_0} \approx -\frac{\theta}{\theta_0} + q_{cl} + q_p. \quad (2-6)$$

In Eq. (2-6), q_{cl} and q_p are the specific water contents in cloud and precipitation, respectively. It should be noted that the water substance variables are the sums of their respective basic states and perturbations. Equation (2-3) can now be rewritten as

$$\frac{\partial\zeta}{\partial t} + \vec{v} \cdot \nabla\zeta - g \frac{\partial}{\partial x} \left(\frac{\theta}{\theta_0} - q_{cl} - q_p \right) = 0. \quad (2-7)$$

The potential temperature perturbation is predicted by the following thermodynamic energy equation

$$\frac{\partial\theta}{\partial t} + \vec{v} \cdot \nabla\theta + w \frac{\partial\theta_0}{\partial z} = \frac{\theta_0}{c_p T_0} [Q_1 + Q_2], \quad (2-8)$$

where c_p is the specific heat at constant pressure, where Q_1 is the latent heat gained or lost when water substance changes phase, and where Q_2 is the loss of heat due to evaporation of rain falling through unsaturated air. These sources will be detailed in 2.3.

Given the temporal history of the water substance fields, Eqs. (2-4), (2-5), (2-7), and (2-8) with proper boundary and initial conditions will permit prediction of the motion and potential temperature fields. 2.4 and 2.5 will summarize the equations governing the water substance fields and the boundary and initial conditions for the model.

2.3 Equations Governing the Macrophysics of Water Substance

By considering the continuity equations for water substance, it can readily be shown [1] that the equations for the mixing ratio of water vapor, q_v , the specific water contents of cloud and precipitation, q_{c1} and q_p --all sums of basic state and perturbation quantities--are

$$\frac{\partial q_v}{\partial t} + \vec{v} \cdot \nabla q_v = \rho_0^{-1} \left(\delta_1 \rho_0 \frac{dq_s}{dt} - \delta_2 S_3 \right), \quad (2-9)$$

$$\frac{\partial q_{c1}}{\partial t} + \vec{v} \cdot \nabla q_{c1} = - \rho_0^{-1} \left(\delta_1 \rho_0 \frac{dq_s}{dt} + \delta_3 S_1 + \delta_4 S_2 \right), \quad (2-10)$$

$$\frac{\partial q_p}{\partial t} + \vec{v} \cdot \nabla q_p = \rho_0^{-1} \left(\delta_3 S_1 + \delta_4 S_2 + \delta_2 S_3 - \frac{\partial}{\partial z} (\rho_0 q_p v) \right), \quad (2-11)$$

where S_1 , S_2 , and S_3 are source terms. S_1 expresses the conversion of cloud to precipitation; S_2 , the depletion of cloud droplets by collision with falling precipitation (accretion); and S_3 , the gain in water vapor through the evaporation of precipitation falling through unsaturated air. In

Eqs. (2-9), (2-10), and (2-11), δ_i ($i = 1, 2, 3, 4$) are symbols indicating the presence ($\delta_i = 1$) or absence ($\delta_i = 0$) of certain terms. The decision, as to whether each of those terms is present, is based on the following criteria:

$$\begin{aligned} \delta_1 &= 1 & \text{if} & & q_{cl} > 0 & \text{or} & & q_v = q_s & \text{and} & & w > 0 \\ \delta_1 &= 0 & \text{if} & & q_v < q_s & \text{or} & & q_v = q_s & \text{and} & & w \leq 0, \end{aligned} \quad (2-12)$$

$$\begin{aligned} \delta_2 &= 1 & \text{if} & & q_p > 0 & \text{and} & & q_v < q_s \\ \delta_2 &= 0 & \text{if} & & q_p > 0 & \text{and} & & q_{cl} > 0, \end{aligned} \quad (2-13)$$

$$\begin{aligned} \delta_3 &= 1 & \text{if} & & q_{cl} > a \\ \delta_3 &= 0 & \text{if} & & q_{cl} < a \end{aligned} \quad (2-14)$$

$$\begin{aligned} \delta_4 &= 1 & \text{if} & & q_p > 0 & \text{and} & & q_{cl} > 0 \\ \delta_4 &= 0 & \text{if} & & q_p = 0 & \text{or} & & q_{cl} = 0. \end{aligned} \quad (2-15)$$

The sources in Eqs. (2-9), (2-10), and (2-11) are given by

$$S_1 = K(\rho_0 q_{cl} - a) \quad \text{gm cm}^{-3} \text{ sec}^{-1}, \quad (2-16)$$

$$S_2 = 6.98 \times 10^{-10} E n_0^{1/8} \rho_0 q_{cl} (\rho_0 q_p)^{7/8} \quad \text{gm cm}^{-3} \text{ sec}^{-1}, \quad (2-17)$$

$$S_3 = -1.35 \times 10^{-12} n_0^{0.35} \rho_0 (q_s - q_v) (\rho_0 q_p)^{0.65} \quad \text{gm cm}^{-3} \text{ sec}^{-1}. \quad (2-18)$$

In Eqs. (2-9) through (2-18), V is the relative fall speed of precipitation, a is the threshold value of $\rho_0 q_{cl}$ above which a part of the cloud is converted to precipitation by autoconversion, K is the efficiency of the autoconversion process (autoconversion parameter), E is the catch coefficient

expressing the efficiency of the accretion process, n_0 is the number of precipitation particles per unit volume per unit diameter, and q_s is the saturation mixing ratio.

Returning now to the heat sources in Eq. (2-8), the source due to phase change is

$$Q_1 = - L \frac{dq_s}{dt} \quad (2-19)$$

and the sink due to evaporation of precipitation is expressed by

$$Q_2 = L \frac{dq_p}{dt} \quad (2-20)$$

From Eq. (2-20), it can be seen that evaporation of falling precipitation will cause a negative dq_p/dt leading to a decrease in θ . The mode of operation of Q_1 is more clearly seen when dq_s/dt is expressed as in [1],

$$\frac{dq_s}{dt} = - H w, \quad (2-21)$$

where

$$H = \frac{g}{R} \left[\frac{0.622L - c_p T_0}{c_p T_0^2 + \frac{L^2}{R_v} q_{s0}} \right] q_{s0}, \quad (2-22)$$

R is the gas constant for moist air, R_v is the gas constant for water vapor, L is the latent heat of vaporization, and q_{s0} is the basic-state value of q_s . Now by Eq. (2-21), when saturated air is moving upwards, condensation takes place and dq_s/dt is negative making Q_1 a source.

Therefore, making use of the relationship already developed for dq_p/dt with the proper physical conditions imposed, the thermodynamic energy Eq. (2-8) may be rewritten as

$$\frac{\partial \theta}{\partial t} + \vec{v} \cdot \nabla \theta + w \frac{\partial \theta_0}{\partial z} = - \frac{\theta_0 L}{c_p T_0} \left(\delta_1 \frac{dq_s}{dt} - \delta_2 \rho_0^{-1} S_3 \right) . \quad (2-23)$$

A further simplification in the system of equations is possible if Eqs. (2-9) and (2-10) are replaced by

$$\frac{\partial q}{\partial t} + \vec{v} \cdot \nabla q = - \rho_0^{-1} \left(\delta_3 S_1 + \delta_4 S_2 + \delta_2 S_3 \right) , \quad (2-24)$$

$$q = q_v + q_{cl} ; \quad \begin{aligned} q_{cl} &= 0 & \text{if } q \leq q_s \\ q_{cl} &= q - q_s & \text{if } q > q_s \end{aligned} \quad (2-25)$$

Note that, with the prescribed conditions, Eq. (2-25) is a simple method of predicting q_{cl} thereby eliminating the differential Eq. (2-10) for q_{cl} . Another advantage to using Eqs. (2-24) and (2-25) is that in the case of no precipitation, q is conserved, i.e.,

$$\frac{dq}{dt} = 0 . \quad (2-26)$$

The system of equations which must be solved for the shallow convection experiment are (2-4), (2-5), (2-7), (2-11), (2-12) through (2-18) with q_v replaced by q , and (2-21) through (2-25).

2.4 Boundary and Initial Conditions

The initial conditions are that the model atmosphere is at rest and contains neither cloud nor precipitation. A buoyant bubble is introduced at the lower part of the symmetry boundary. A quantitative description of the initial conditions will be presented in Section 4.0 of this report.

The kinematic boundary conditions follow from the geometry of the model. The rigid wall and symmetry conditions require that motion normal to the walls

and the symmetry plane ($x = 0$) vanish. Also it shall be required that $q_p = 0$ at the upper boundary. These conditions are shown in Fig. 1. Mathematically, the boundary conditions are

$$\begin{aligned} \text{at } z = 0 : \quad & \psi = \zeta = 0 ; \\ \text{at } z = H : \quad & \psi = \zeta = q_p = 0 ; \\ \text{at } x = 0, L : \quad & \psi = \zeta = 0 . \end{aligned} \quad (2-27)$$

With these boundary conditions, the system of equations is complete.

2.5 The Diagnostic Pressure Equation

The incompressibility feature of the model [see Eq. (2-1)] readily permits the derivation of a diagnostic equation for the dynamic pressure. The driving forces of the model are the buoyancy force and the dynamic pressure. Therefore, it is useful to obtain the pressure field in order to gain further insight into the dynamics of shallow convection as can be seen in the latest report [4]. The departure of the dynamic pressure from the hydrostatic pressure has been demonstrated for both the dry convection [2] and the moist convection [4] experiments.

The diagnostic pressure equation is obtained by taking the divergence of the equation of motion (2-2) and applying the continuity equation (2-1) yielding

$$\nabla^2 p = g \frac{\partial}{\partial z} \rho_0 \left(\frac{\theta}{\theta_0} - q_{cl} - q_p \right) + \nabla \cdot (\rho_0 \vec{v} \cdot \nabla \vec{v}) = 0 . \quad (2-28)$$

The boundary conditions appropriate to Eq. (2-28) follow from application of the kinematic boundary conditions (2-27) to the equation of motion (2-2). Namely, they are that the pressure is hydrostatic at the upper and lower

boundaries, and that the pressure gradients normal to the lateral boundaries vanish. Mathematically

$$\begin{aligned} \text{at } z = 0, H : \quad \frac{\partial p}{\partial z} &= g \rho_0 \left(\frac{\theta}{\theta_0} - q_{cl} - q_p \right) ; \\ \text{at } x = 0, L : \quad \frac{\partial p}{\partial x} &= 0 . \end{aligned} \quad (2-29)$$

Given the complete system of equations summarized in the previous sections, and the diagnostic pressure equation with its associated boundary conditions, the shallow convection fields of motion, potential temperature, water substance, and dynamic pressure may be determined for any time.

3.0 SUMMARY OF FINITE-DIFFERENCE APPROXIMATIONS

Consider finite increments $(\Delta x, \Delta z)$ on the coordinate axes, and let there be a mesh of points determined by ordered sums of these finite increments. It follows that the coordinates of any point in the mesh are $m\Delta x, n\Delta z$ ($m = 1, 2, \dots, M, n = 1, 2, \dots, N$). Analogously, discrete values of time are considered as ordered sums of a finite time increment Δt ($l = 0, 1, 2, \dots$). Then the system of equations summarized in the preceding sections may be approximated by finite-difference equations defined on the mesh. The finite-difference equations may be numerically integrated with respect to time between successive time steps. The resulting system of numerically integrated equations may be solved for the dependent variables at any time step. Any function, $f(x, z, t)$, defined on the mesh, will have the value $f_{m,n}^l$ at the point $(m\Delta x, n\Delta z, l\Delta t)$. Any basic-state variable $h_0(z)$, being a function of z alone, will have the value h_{0m} at the point $(n\Delta x, m\Delta z, l\Delta t)$.

3.1 Finite-Difference Equations Used for the Interior Points

All of the following equations are used at the interior mesh points for all time steps except the initial one. Therefore, the domain of these equations is $2 \leq m \leq M-1, 2 \leq n \leq N-1, l \geq 1$.

3.1.1 The centered-difference approximations

The equations used to approximate Eq. (2-4) to determine the wind from the stream function are

$$u_{m,n}^l = - \frac{\psi_{m,n+1}^l - \psi_{m,n-1}^l}{2\Delta z}, \quad (3-1a)$$

$$w_{m,n}^l = \frac{\psi_{m+1,n}^l - \psi_{m-1,n}^l}{2\Delta x}. \quad (3-1b)$$

Equation (2-5) is used to solve for the stream function given the vorticity field and is approximated by

$$\frac{\psi_{m+1,n}^{\ell} - 2\psi_{m,n}^{\ell} + \psi_{m-1,n}^{\ell}}{(\Delta x)^2} + \frac{\psi_{m,n+1}^{\ell} - 2\psi_{m,n}^{\ell} + \psi_{m,n-1}^{\ell}}{(\Delta z)^2} = \zeta_{m,n}^{\ell} \quad (3-2)$$

The vorticity Eq. (2-7) is approximated by a modified centered-difference approximation. The horizontal derivative of $[(\theta/\theta_0) - q_{cl} - q_p]$ is approximated by a vertically weighted average of centered differences. The equation is numerically integrated from $(\ell - 1)\Delta t$ to $(\ell + 1)\Delta t$. With these modifications, the equation used to predict the vorticity at $(\ell + 1)\Delta t$ is

$$\begin{aligned} \zeta_{m,n}^{\ell+1} = & \zeta_{m,n}^{\ell-1} - \frac{\Delta t}{\Delta x} \left[(u\zeta)_{m+1,n}^{\ell} - (u\zeta)_{m-1,n}^{\ell} \right] - \frac{\Delta t}{\Delta z} \left[(w\zeta)_{m,n+1}^{\ell} \right. \\ & \left. - (w\zeta)_{m,n-1}^{\ell} \right] + \frac{g\Delta t}{4\Delta x} \left[\frac{\theta_{m+1,n+1}^{\ell} - \theta_{m-1,n+1}^{\ell}}{\theta_{0,n+1}} \right. \\ & + 2 \left(\frac{\theta_{m+1,n}^{\ell} - \theta_{m-1,n}^{\ell}}{\theta_{0,n}} \right) + \left. \frac{\theta_{m+1,n-1}^{\ell} - \theta_{m-1,n-1}^{\ell}}{\theta_{0,n-1}} \right] \\ & - (\bar{q}_{m+1,n+1}^{\ell} - \bar{q}_{m-1,n+1}^{\ell}) - 2(\bar{q}_{m+1,n}^{\ell} - \bar{q}_{m-1,n}^{\ell}) \\ & \left. - (\bar{q}_{m+1,n-1}^{\ell} - \bar{q}_{m-1,n-1}^{\ell}) \right] \end{aligned} \quad (3-3)$$

where $\bar{q}_{m,n}^{\ell} = q_{clm,n}^{\ell} + q_{pnm,n}^{\ell}$. An additional change made in Eq. (2-7) to arrive at (3-3) is the replacement of the advection of vorticity $\vec{v} \cdot \nabla \zeta$ by the divergence of vorticity flux $\nabla \cdot \zeta \vec{v}$. The equivalence of these two terms is clear in the case of non-divergent flow.

The diagnostic pressure Eq. (2-28) is modified by replacing the last term on the left side by its stream function equivalent, thus

$$\nabla \cdot \rho_0 (\vec{v} \cdot \nabla \vec{v}) = 2\rho_0 \left[\left(\frac{\partial \psi^2}{\partial x \partial z} \right)^2 - \frac{\partial^2 \psi}{\partial x^2} \frac{\partial^2 \psi}{\partial z^2} \right] \quad (3-4)$$

With this substitution, Eq. (2-28) is approximated by

$$\begin{aligned} & \frac{p_{m+1,n} - 2p_{m,n} + p_{m-1,n}}{(\Delta x)^2} + \frac{p_{m,n+1} - 2p_{m,n} + p_{m,n-1}}{(\Delta z)^2} \\ &= \frac{g}{2\Delta z} \left\{ \rho_{0n+1} \left[\frac{\theta_{m,n+1}^{\ell}}{\theta_{0n+1}^{\ell}} - \bar{q}_{m,n+1}^{\ell} \right] - \rho_{0n-1} \left[\frac{\theta_{m,n-1}^{\ell}}{\theta_{0n-1}^{\ell}} - \bar{q}_{m,n-1}^{\ell} \right] \right\} \\ &+ 2\rho_{0n} \left\{ \frac{1}{4(\Delta x)^2 (\Delta z)^2} \left[(\psi_{m+1,n+1}^{\ell} - 2\psi_{m,n}^{\ell} + \psi_{m-1,n-1}^{\ell}) (\psi_{m-1,n+1}^{\ell} \right. \right. \\ &\left. \left. - 2\psi_{m,n}^{\ell} + \psi_{m+1,n-1}^{\ell}) - (\psi_{m,n+1}^{\ell} + \psi_{m,n-1}^{\ell} - \psi_{m-1,n}^{\ell} - \psi_{m+1,n}^{\ell})^2 \right] \right\} \quad (3-5) \end{aligned}$$

The term involving the stream function in Eq. (3-5) is not obtained by normal centered differences. It has been found advantageous (see [2]) to take centered differences along the diagonals of the established mesh rather than along the axes. This procedure is valid only if $\Delta x = \Delta z$, in which case, the mesh length is $\sqrt{2} \cdot \Delta x$ rather than Δx and/or Δz . The advantage of using this technique is that it insures consistent truncation of both terms of the right-hand side of Eq. (3-4).

3.1.2 The Lax-Wendroff scheme applied to the equations for heat and water substance

It should be noted that the Eqs. (2-23), (2-11), (2-21), and (2-24), used to predict θ , q_p , q_s , and q , respectively, are all of the form

$$\frac{\partial f}{\partial t} + \nabla \cdot (f\vec{v}) = S,$$

where f symbolizes the dependent variable, and S is the totality of sources and sinks. These equations are approximated by the two-step Lax-Wendroff

scheme. For the sake of brevity, the scheme will be described for the general equation above. For odd time steps, the approximation is

$$f_{m,n}^{l+1} = \bar{f}_{m,n}^l + \frac{\Delta t}{2\Delta x} \left[(fu)_{m-1,n}^l - (fu)_{m+1,n}^l \right] + \frac{\Delta t}{2\Delta z} \left[(fw)_{m,n-1}^l - (fw)_{m,n+1}^l \right] + \Delta t \cdot S_{m,n}^l, \quad (3-6)$$

in which

$$\bar{f}_{m,n}^l = \frac{f_{m+1,n}^l + f_{m-1,n}^l + f_{m,n+1}^l + f_{m,n-1}^l}{4}. \quad (3-7)$$

In the case of variables which are retained as the sum of the basic state and the perturbation, e.g., q , in order to avoid smoothing the basic state, the following expression is used in place of Eq. (3-7),

$$\bar{f}_{m,n}^l = \frac{f_{m+1,n}^l + f_{m-1,n}^l + f_{m,n+1}^l + f_{m,n-1}^l - 2f_{0n}^l - f_{0n+1}^l - f_{0n-1}^l}{4} + f_{0n}^l. \quad (3-8)$$

For even time steps, the approximation is

$$f_{m,n}^{l+1} = f_{m,n}^{l-1} + \frac{\Delta t}{\Delta x} \left[(fu)_{m-1,n}^l - (fu)_{m+1,n}^l \right] + \frac{\Delta t}{\Delta z} \left[(fw)_{m,n-1}^l - (fw)_{m,n+1}^l \right] + 2\Delta t \cdot S_{m,n}^l. \quad (3-9)$$

In application to the particular equations in θ , q_p , q_s , and q , f needs only to be replaced by the proper symbol and S by the appropriate source-sink terms.

This completes the finite difference approximations to the system of continuous equations required at the interior points of the finite mesh.

3.2 Boundary Conditions

The boundary conditions, Eq. (2-27), for the vorticity and stream function fields can be readily expressed in finite difference form. They are

$$\begin{aligned} \zeta_{1,n}^l &= \zeta_{M,n}^l = \zeta_{m,1}^l = \zeta_{m,N}^l = 0, \\ \psi_{1,n}^l &= \psi_{M,n}^l = \psi_{m,1}^l = \psi_{m,N}^l = 0. \end{aligned} \quad (3-10)$$

Application of these conditions to Eq. (2-4) leads to one sided difference approximations

$$\begin{aligned} w_{1,n}^l &= \frac{\psi_{2,n}^l}{\Delta x}, & w_{M,n}^l &= -\frac{\psi_{M-1,n}^l}{\Delta x}; \\ u_{m,1}^l &= -\frac{\psi_{m,2}^l}{\Delta z}, & u_{m,N}^l &= \frac{\psi_{m,N-1}^l}{\Delta z}. \end{aligned} \quad (3-11)$$

These conditions are explicitly applied to the stream function Eq. (3-1) and the vorticity Eq. (3-2).

The boundary conditions, Eq. (2-29), in finite difference form are

$$\left. \begin{aligned} p_{m,N}^l &= p_{m,N-1}^l + g \cdot \Delta z \cdot \rho_{0N} \left(\frac{\theta_{m,N}}{\theta_{0N}} - \bar{\alpha}_{m,N}^l \right), \\ p_{m,1}^l &= p_{m,2}^l - g \cdot \Delta z \cdot \rho_{01} \left(\frac{\theta_{m,1}}{\theta_{01}} - \bar{\alpha}_{m,1}^l \right), \\ p_{1,n}^l &= p_{2,n}^l, \\ p_{M,n}^l &= p_{M-1,n}^l. \end{aligned} \right\} \quad (3-12)$$

For heat and water substance, the kinematic boundary conditions, Eq. (2-27), must be applied to the respective differential equations. The resulting differential equations may be of either of the two following forms:

$$\frac{\partial f}{\partial t} + v_1 \frac{\partial f}{\partial x_1} = S, \quad (3-13)$$

or

$$\frac{\partial f}{\partial t} + \frac{\partial f v_1}{\partial x_1} - f \frac{\partial v_1}{\partial x_1} = S, \quad (3-14)$$

where the subscript 1 indicates the direction parallel to the boundary under consideration. Thus, for the lateral boundaries, $v_1 \equiv w$, $x_1 \equiv z$, and for the upper and lower boundaries, $v_1 \equiv u$, $x_1 \equiv x$.

Consider first the Lax-Wendroff scheme for Eq. (3-13). For brevity, we will demonstrate the approximations only for the lower boundary. To determine the approximation for any other boundary, one need only substitute the proper subscripts and wind components. The approximation for odd time steps is

$$f_{m,1}^{l+1} = \bar{f}_{m,1}^l + \frac{\Delta t}{2\Delta x} \bar{u}_{m,1}^l (f_{m-1,1}^l - f_{m+1,1}^l) + \Delta t \cdot S_{m,1}^l, \quad (3-15)$$

where

$$\bar{f}_{m,1}^l = \frac{f_{m+1,1}^l + f_{m-1,1}^l}{2}, \quad (3-16)$$

and the expression for $\bar{u}_{m,1}^l$ is the same as (3-16) with f replaced by u .

For even time steps, the approximation is

$$f_{m,1}^{l+1} = f_{m,1}^{l-1} + \frac{\Delta t}{\Delta x} \bar{u}_{m,1}^l (f_{m-1,1}^l - f_{m+1,1}^l) + 2\Delta t \cdot S_{m,1}^l. \quad (3-17)$$

This form is applied to θ .

Now consider the Lax-Wendroff scheme applied to Eq. (3-14). For odd time steps, the approximation is

$$f_{m,1}^{l+1} = \bar{f}_{m,1}^l + \frac{\Delta t}{2\Delta x} \left[(fu)_{m-1,1}^l - (fu)_{m+1,1}^l + \bar{f}_{m,1}^l (u_{m+1,1}^l - u_{m-1,1}^l) \right] + \Delta t \cdot S_{m,1}^l. \quad (3-18)$$

For even time steps, the approximation is

$$f_{m,1}^{l+1} = f_{m,1}^{l-1} + \frac{\Delta t}{\Delta x} \left[(fu)_{m-1,1}^l - (fu)_{m+1,1}^l - \bar{f}_{m,1}^l (u_{m+1,1}^l - u_{m-1,1}^l) \right] + 2\Delta t \cdot S_{m,1}^l \quad (3-19)$$

This form is applied to q and q_g , and to q_p at the lateral boundaries.

At the upper boundary, according to the boundary conditions, Eq. (2-29), q_p is zero. At the lower boundary, a special scheme is employed to solve for q_p . The form of the differential equation is the same as Eq. (3-13) where $-(\partial/\partial z)(Vq_p)$ is included in S . Instead of the two-step Lax-Wendroff scheme, a forward time difference scheme is used. One other change is that upwind differences and averages are used to approximate the advection term rather than the centered differences which are employed in all other approximations. With these changes, the approximations are: if $u_{m,1} > 0$, then

$$q_{p,m,1}^{l+1} = q_{p,m,1}^l - \frac{\Delta t}{\Delta x} \left(\frac{u_{m,1}^l + u_{m-1,1}^l}{2} \right) (q_{p,m,1}^l - q_{p,m-1,1}^l) + \Delta t \cdot S_{m,1}^l ; \quad (3-20)$$

and, if $u_{m,1} \leq 0$, then

$$q_{p,m,1}^{l+1} = q_{p,m,1}^l - \frac{\Delta t}{\Delta x} \left(\frac{u_{m,1}^l + u_{m+1,1}^l}{2} \right) (q_{p,m+1,1}^l - q_{p,m,1}^l) + \Delta t \cdot S_{m,1}^l \quad (3-21)$$

This completes the incorporation of the boundary conditions into the finite difference system.

3.3 Initial Time Step Approximation

The finite difference form for the vorticity Eq. (3-3) involves the previous time step. This cannot be done initially so the following approximation is used to compute the vorticity field:

$$\zeta_{m,n}^1 = \frac{g \cdot \Delta t}{2 \cdot \Delta x} \left(\frac{\theta_{m+1,n}^0 - \theta_{m-1,n}^0}{\theta_{0n}^0} \right) \quad (3-22)$$

The finite difference form, Eq. (3-6), applies to the remaining prediction equations.

This concludes the summary of the finite difference approximations for the shallow moist convection simulation model. The next section describes the initial data required for the experiments.

4.0 THE INITIAL DATA

The initial data required for a moist convection simulation are the one-dimensional basic-state fields of potential temperature θ_0 , density, ρ_0 , temperature T_0 , pressure p_0 , saturation vapor pressure e_{s0} , and relative humidity r_0 , and the two-dimensional perturbation field of potential temperature corresponding to the buoyant bubble. The fields of T_0 , p_0 , e_{s0} , and r_0 are used to compute the initial fields of q_g and q_v .

Initially the model is assumed to be saturated and to have, very nearly, a moist adiabatic stratification. The physical variables which characterize this basic state are presented in Table 1. These are the same values which have been given in previous reports [3, 4].

The buoyant bubble is the same as used in all previous experiments [2, 3, 4]. It is shown in Fig. 2 as a potential temperature perturbation.

Table 1

Basic-state distribution with height of potential temperature, temperature, density, pressure, saturation vapor pressure, and relative humidity.

$z(10^2\text{m})$	$\theta_0(^{\circ}\text{K})$	$T_0(^{\circ}\text{K})$	$\rho_0(10^{-3}\text{g/cm}^3)$	$p_0(\text{mb})$	$e_{s_0}(\text{mb})$	$r_0(\%)$
0	297.00	297.00	1.160	1000.0	29.83	100
1	297.53	296.58	1.149	989.0	29.12	100
2	298.06	296.16	1.138	978.0	28.43	100
3	298.58	295.74	1.127	967.0	27.58	100
4	299.22	295.32	1.114	955.0	26.92	100
5	299.80	294.90	1.103	944.0	26.27	100
6	300.37	294.48	1.092	933.0	25.64	100
7	300.88	294.06	1.082	923.0	25.01	100
8	301.48	293.64	1.071	912.0	24.26	100
9	301.99	293.22	1.061	902.0	23.66	100
10	302.52	292.80	1.051	892.0	23.09	100
11	303.05	292.38	1.040	882.0	22.52	100
12	303.61	291.96	1.030	872.0	21.96	100
13	304.16	291.54	1.020	862.0	21.29	100
14	304.74	291.12	1.010	852.0	20.76	100
15	305.35	290.70	0.999	842.0	20.24	100
16	305.96	290.28	0.989	832.0	19.74	100
17	306.56	289.86	0.979	822.0	19.25	100
18	307.07	289.44	0.970	813.0	18.64	100
19	307.72	289.02	0.959	803.0	18.17	100
20	308.25	288.60	0.950	794.0	17.71	100
21	308.81	288.18	0.941	785.0	17.26	100
22	309.49	287.76	0.930	775.0	16.83	100
23	310.07	287.34	0.921	766.0	16.29	100
24	310.68	286.92	0.911	757.0	15.87	100
25	311.28	286.50	0.902	748.0	15.47	100
26	311.91	286.08	0.893	739.0	15.07	100
27	312.54	285.66	0.883	730.0	14.68	100
28	313.05	285.24	0.875	722.0	14.20	100
29	313.73	284.82	0.865	713.0	13.83	100
30	314.26	284.40	0.857	705.0	13.47	100

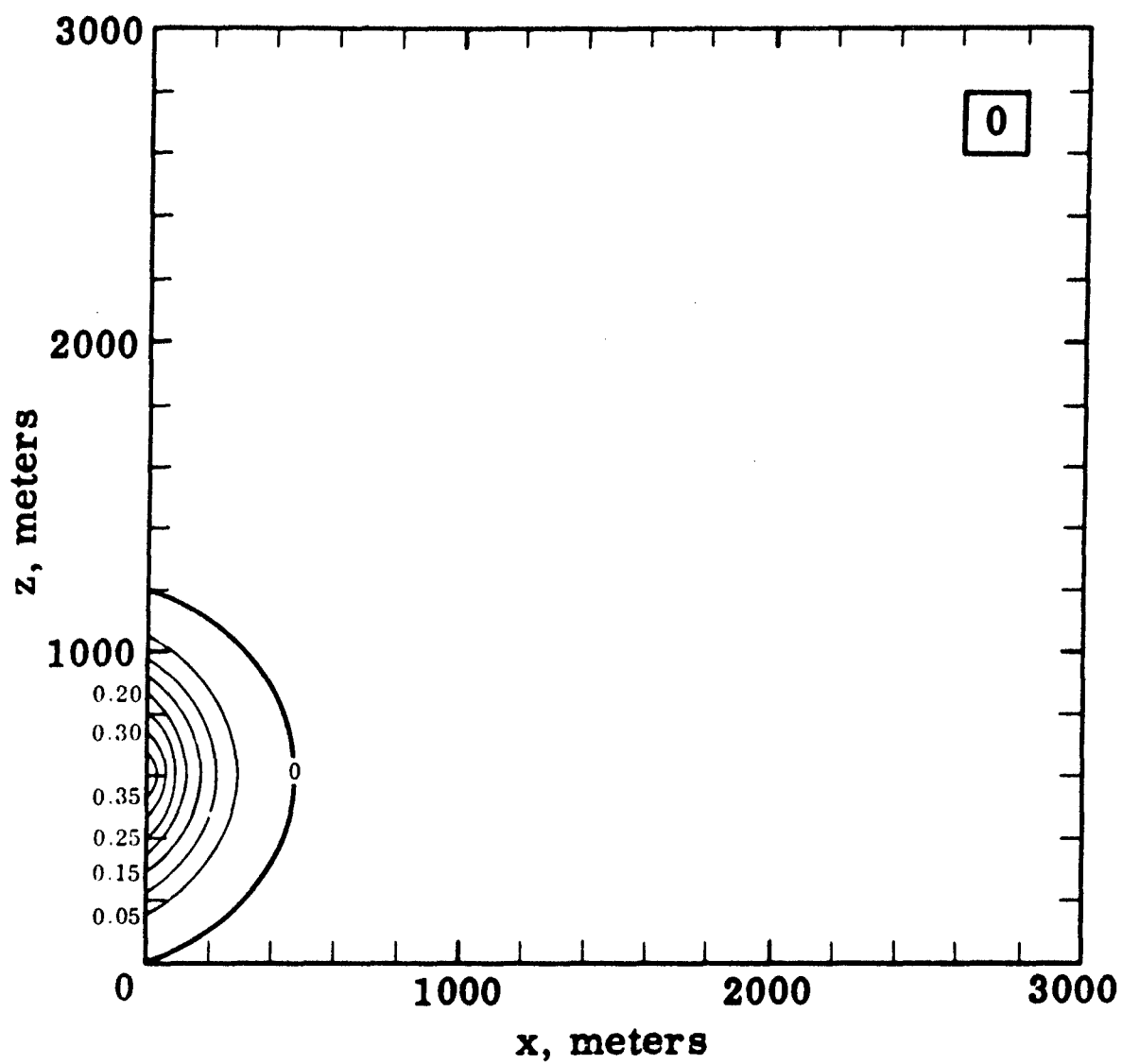


Fig. 2. Initial potential temperature perturbation in $^{\circ}\text{C}$.

5.0 PROGRAM DESCRIPTION

This section describes the current computer program used for the numerical simulation experiments in moist, shallow convection. The most meaningful type of program description is in the form of flow diagrams given in Appendix B. From these, the details of the logical flow within the program may be followed.

5.1 Input

The required input to the program can be divided into three categories: control variables, program constants, and initial fields. The latter were summarized in Section 4.0. The others will be discussed below.

5.1.1 Control variables

The variables, which are used to control certain internal operations of the program, permit flexibility in the computations and the resulting output. By being able to set these variables at the outset, one is able to significantly modify the computational scheme without changing the existing program.

The control variables in the present program are given in Table 2. All of the control variables are punched on one input card.

Table 2
Control variables input to the program

Variable Program Identification	Controls
MX	Number of horizontal grid points
NZ	Number of vertical grid points
NTS	Number of time steps
IDTMX	Maximum allowable time steps
ITST	Frequency of relaxing the dynamic pressure field. Pressure relaxation always occurs initially and at end of first time step, i.e., if ITST = 3, relaxation occurs at time step 0, 1, 3, 6, 9, ...
JTST	Frequency of printing output. Operation equivalent to ITST
IMØ	Dry (IMØ = 0) or moist (IMØ = 1) convection simulation

5.1.2 Program constants

The program constants are used in the computations. By changing these constants, except for CVN1 and CVN2, the physics or geometry of the experiments are modified. The program constants are given in Table 3.

Table 3
Program constants input to the program

Program Constant	Definition
CL	Horizontal extent of model
CH	Vertical extent of model
GV	Viscosity coefficient. The model has so far been run with $GV = 0$ (non-viscous)
CVN1	Convergence criterion for stream function relaxation
CVN2	Convergence criterion for dynamic pressure relaxation
RV	Water vapor gas constant (R_v)
EL	Latent heat of vaporation (L)
CP	Specific heat at constant pressure (c_p)
R	Moist air gas constant (R)
ZN0	Number of precipitation particles (n_0)
A	Threshold value for autoconversion (a)
ZK	Cloud autoconversion parameter (K)
E	Precipitation catch coefficient (E)
V	Relative precipitation fall speed (V)

5.1.3 Input format

All of the input is on punched cards to be read by the computer. The format of the input cards may be found in Table 4.

Card 1 is a recovery control card. The details of its function and format are discussed in 5.4.2. It can be seen from Table 4 that a standard moist convection experiment requires 237 cards of input data. It should be noted that the program can be used to simulate dry convection, i.e., convection in

which all water substance is ignored. As shown in Table 2, the control variable for a dry convection run is set equal to 1. Therefore, input card 5 must be altered accordingly. Also, input cards 204-237 are not part of the input required for a dry convection experiment.

Table 4
Input card format

Input Card Number	Contents	Fortran Format
1	See 5.4.2	---
2	Comments to identify the experiment; used for output	12A6
3	CL, CH, GV	6F12.4
4	Blank, CVN1, CVN2	5F12.4
5	NZ, MX, NTS, IDTMX, ITST, JTST, IMØ	7I5
6-11	Basic potential temperature field, θ_{0n}	6F12.4
12-17	Basic density field, ρ_{0n}	6F12.4
18-203	"Bubble" (potential temperature perturbation field $\theta'_{m,n}$)	6F12.4
204	RV, EL, CP, R	4F12.4
205	ZNØ, A, ZK, E	4F12.4
206	V	1F12.4
207-237	$T_n, p_n, e_{s,n}, r_n$	4F12.4

5.2 Internal Operations

The internal operations of the computer program have been separated into subroutines each of which performs a specialized set of computations and/or operations. The main program (MAIN) controls the sequence in which the subroutines are called upon, thereby directing the general flow of the computations. Each of these aspects of the computer program are summarized below.

5.2.1 Subroutine operations

Within each subroutine, a block of operations or computations is performed. Table 5 states the purpose of each subroutine.

Table 5
Purpose of program subroutines

Subroutine Fortran Name	Purpose
PRTIN	Prints the "dry" input to the moist or dry convection simulations
MØISIN	Reads and prints "moist" input; computes and prints initial q_s - and q -fields
RELAX1	Performs relaxation of stream function field; selectively prints convergence information
RELAX2	Performs relaxation of dynamic pressure field and prints convergence information
HYPRES	Computes hydrostatic pressure (P2)
CSBR	Computes source function for θ -prediction
PRDCTM	Computes source functions for and controls prediction of q_p , q_s , and q
PREDIN	Predicts values of q_p , q_s , and q for interior points
PREDUL	Predicts upper and lower boundary values of q_p , q_s , and q
PREDLR	Predicts lateral boundary values of q_p , q_s , and q
EXCNG	Selectively controls flow of arrays to and from auxiliary storage
SMØØTH	Transfers fields from dummy array (DUMA) to proper array
DUMP	Prints source functions for θ and q_p
SUMPK	Computes and prints space averaged potential and kinetic energy
SUMTB	Computes and prints space averaged potential temperature
PRTØUT	Prints the fields of potential temperature perturbation, stream function, vorticity, dynamic and hydrostatic pressure, specific water content of cloud and precipitation, saturation mixing ratio, and total specific water substance (q)

Some of these subroutines are called every time step while others are selectively called, based on input values of certain control variables, namely ITST and JTST. The subroutines which are selectively called are DUMP, RELAX2, HYPRES, SUMPk, SUMTB, and PRTOUT. There are also two subroutines which are called only at the initial time step, namely PRTIN and MOISIN.

5.2.2 General flow

This section will merely summarize the general flow. The summary will neglect the variations under the several recovery options as these will be discussed in 5.4. The details of the general flow are shown in the flow diagram of the MAIN program, Fig. A-1 (see Appendix B).

The general flow of the computations are summarized below:

1. Read input cards 1 through 203.
2. Compute program constants.
3. Call PRTIN.
4. If moist convection - call MOISIN.
5. Call SUMPk, SUMTB, RELAX2, HYPRES, PRTOUT.
6. Compute initial vorticity field.
7. Call RELAX1.
8. Compute wind fields (u and w) from stream function field.
9. If moist convection - call CSBR.
10. Compute potential temperature for odd time steps.
11. Compute potential temperature for even time steps.
12. If moist convection - call PRDCTM.
13. If this time step is to be printed - call SUMPk, SUMTB, RELAX2, HYPRES, PRTOUT.
14. Compute and test length of next time step.

} Performed
alternately

15. Compute new vorticity field.

16. If this is not last time step - return to step 7.

17. STOP.

As pointed out in 5.1.1, the decisions which determine the specific flow (dry or moist convection, print or non-print time step, last time step) are directed by the input control variables.

This concludes the summary of the internal operations of the computer program. The following sections will discuss the output.

5.3 Output

There are three types of output from the program. In order of importance, they consist of:

- 1) the physical and kinematic fields,
- 2) fields or values which either measure the efficiency of the computations or provide additional details of the physical properties of the model (printed by the RELAX1, RELAX2, DUMP, SUMP, and SUMTB subroutines), and
- 3) the input data and the initially computed fields (printed by the PRTIN and M0ISIN subroutines).

5.3.1 Form

The primary output consists of successively printed fields of θ , ψ , ζ , dynamic and hydrostatic pressure, q_{cl} , q_p , q_s , and q . Along the margins of each field, the x and z indices are printed.

The secondary output takes several forms. The convergence information printed out by RELAX1 and RELAX2 consists of three columns of figures corresponding respectively to the number of each iteration, the maximum residual of that iteration, and the departure from the convergence criterion. Thus, a summary of each relaxation is printed until convergence or 50 iterations have occurred. The output from DUMP consists of printouts of source func-

tion fields for θ and q_p . The output from SUMPK consists of three numbers, namely the space averaged potential, P , and kinetic, K , energies and the difference $P - K$. The final secondary output comes from SUMTB and consists of a single number, the space averaged potential temperature.

The initial output from PRTIN and MØISIN consists of an orderly summary of the input data, as well as the initial fields of θ , q_s , and q .

5.3.2 Controls and options available

The controls and options available for the output, at present, are centered in the two control variables, ITST and JTST. By suitable choice of ITST, one can specify the frequency of relaxing the dynamic pressure field and computing the hydrostatic pressure field as well as the printing of both pressure fields. The frequency with which all other primary and secondary output are printed is established by the value input for JTST. Therefore, the output options, presently available, consists of a predetermined fixed frequency of pressure field output and a predetermined fixed frequency of other primary and secondary output. These two frequencies can be either the same or different. The modes of operation of ITST and JTST were given in Table 2.

5.3.3 Anticipated changes

There are several changes in the output which are anticipated.

These are:

- 1) water substance budget,
- 2) changes in q_p output at the bottom of symmetry boundary, and
- 3) more output options.

The first change will be made shortly. The water substance budget will consist of the space averages of water vapor density, liquid cloud density,

precipitation density, and cumulative precipitation reaching the lower boundary. All of these will be computed at selected time steps to evaluate the degree of computational agreement with the water substance continuity equation.

Presently, the corner values of q_p remain zero for all time. Clearly, the value at the bottom of the symmetry boundary should eventually become the maximum value in the q_p field. A scheme to determine q_p at that point will be developed in the near future.

The third anticipated change is more speculative than the others. Undoubtedly, it would be desirable if the output options were more flexible than they are in the present program. If suitable criteria can be established, it would be most advantageous if the printing frequency could be internally controlled. The criteria would be used to determine significant changes in the model. Then, detailed output could be obtained when significant changes were occurring, whereas a more general output would be printed at a predetermined frequency. If these criteria can be established, more flexible output options will be developed.

This completes the changes in output which are presently anticipated. The next section will discuss the recovery capability of the program.

5.4 Recovery

The recovery feature is the most recent change that has been made in the program. This feature permits resuming a completed convection experiment from some predetermined time step under various values of the physical parameters. The most obvious advantage in having this option available is the capability of assessing the sensitivity of parallel experiments to varying physical conditions.

5.4.1 Method

By a suitable initial input card, a given convection experiment can be run so that a recovery can be accomplished from specified time steps. This is achieved by storing on tape the arrays of all unknowns, as well as the necessary program constants, for the fixed-interval time steps specified on the initial input card.

To recover from a previous convection simulation, by including a suitable initial input card, the recovery tape is searched until the data for the predetermined time step are found. Then the following sequence occurs.

1. The data is read from the recovery tape into the computer's internal storage.
2. The physical constants (input cards 2 through 5, 204 through 206) are then read into internal storage.
3. The general flow is started at step 7 (see 5.2.2).
4. The experiment is run to completion.

The details of this sequence may be found in the flow diagram of MAIN (Fig. A-1). Note that step 2 above is the point at which the physical conditions for the recovery simulation may be changed from those of the original simulation experiment.

5.4.2 Available options and associated input controls

All of the recovery options are guided by the values of the control variables on the initial input card. There are four recovery control variables, namely

- INT - designation of recovery tape unit
- NTPS - number of time periods to be skipped for recovery tape input
- IDINC - fixed-interval for selecting time steps for recovery output
- IBTS - starting time step for recovery input.

The FORTRAN format of the first input card is 6I3, 9A6; and the contents are INT, NTPS, IDINC, IBTS, blank, blank, recovery comments.

The four available recovery options with the associated values of the control variables are as follows.

Option 1 - No recovery input or output

INT = IBTS = 0

Option 2 - Store necessary data on recovery tape every T time step starting at time step 0 .

INT = any number between 8 and 26

NTPS = 0

IDINC = T

IBTS = 0

Option 3 - Recover from previous experiment where IDINC = T_0 at time step TS and store necessary new data on recovery tape every T_n time steps (Note: T_n may be different than T_0).

INT = any number between 8 and 26

NTPS = TS/T_0

IDINC = T_n

IBTS = TS

Option 4 - Recover from previous experiment where IDINC = T_0 at time step TS , but do not store any data for future recovery

INT = any number between 8 and 26

NTPS = TS/T_0

IDINC \geq NTS (number of time steps in experiment)

IBTS = TS

The details of the mode of operation under each of these operations may be found in the MAIN flow diagram (Fig. A-1).

6.0 CONCLUSIONS

This report summarizes the convection model which has been developed at The Travelers Research Center, Inc. for the sponsoring agency. The primary purpose of the report is to give a detailed description of the computer program which numerically integrates the modelling equations. The concluding remarks will discuss the present status of the computer program and the future plans for its use.

6.1 Present Status

The results summarized in the last report under this contract [4] were obtained using the program described in this report on the IBM 7094 system. Since that time, the program has been modified so that it is fully operable on the UNIVAC 1108 system. From the timing obtained on trial runs, it is anticipated that, to perform a simulation of 10 minutes of moist convection, will require approximately 22 minutes of computations on the 1108 system. This is approximately three times faster than the IBM 7094 requires for the same simulation.

Of the total internal storage available for program instructions, approximately 70% remains available after the present program is stored. Also, approximately 35% of the data storage remains available when the present program is running. A characteristic feature of UNIVAC 1108 is that these two types of storage are interchangeable only at the sacrifice of speed in computations. If this is done, a considerable increase in data storage is possible, and expansion of the present program is under consideration.

6.2 Future Plans

The future plans for this project may be summarized in three separate categories:

- 1) computational modifications,
- 2) changes in basic state, and
- 3) experiments.

Naturally, there is some interdependence between the categories.

The plans for computational modification are:

- 1) computation of a water substance balance,
- 2) computation of variable q_p values at lower corner of symmetry boundary,
- 3) correction of space averaged potential energy, and
- 4) computation of a variable precipitation fall speed.

The first three modifications have been discussed in foregoing sections of this report. The last modification represents a change of the present method of using a constant fall speed. A suitable formula obtained elsewhere, relating fall speed to appropriate cloud physics parameters, will be used in the future.

The plans for changes in the basic state are:

- 1) a non-saturated lower layer, and
- 2) a very stable, non-saturated upper layer.

These two changes are quite simple to accomplish. Moreover, they produce a basic state more comparable to the climatological tropical atmosphere.

The anticipated experiments include:

- 1) by using recovery, comparing the effects of suppression and non-suppression of precipitation,
- 2) studying the effects of the stable top layer, and
- 3) studying the effects of the evaporation of precipitation in the non-saturated layer below the cloud base.

The next report will discuss the results of the experiments completed in the next six-month period.

7.0 LITERATURE CITED

- 1 Arnason, G. and E.A. Newburg, 1964: Relationships Between Tropical Precipitation and Kinematic Cloud Models. Report No. 6, Contract DA 36-039 SC 89099, The Travelers Research Center, Inc.
- 2 _____, and _____, 1966: Relationships Between Tropical Precipitation and Kinematic Cloud Models. Report No. 8, Contract DA 28-043 AMC 01219(E), The Travelers Research Center, Inc.
- 3 _____, and A.F. Saunders, 1966: Relationships Between Tropical Precipitation and Kinematic Cloud Models. Final Report No. 9, Contract DA 28-043 AMC 01219(E), The Travelers Research Center, Inc.
- 4 _____, and _____, 1966: Relationships Between Tropical Precipitation and Kinematic Cloud Models. Semi-annual Report No. 1, Contract DA 28-043 AMC 02192(E), The Travelers Research Center, Inc.

APPENDIX A

APPENDIX A

List of Symbols

With the exception of n , subscript 0 on any symbol is used in this report to designate the basic state of the variable represented by the symbol. Superscript i and subscripts m and n on any symbol in this report are used to denote the value of the variable represented by the symbol at a point in the finite difference mesh with i the time index, m the x-index, and n the z-index. Table 3 gives the alternative symbols used in the program for certain of the symbols given below.

a	threshold value for q_{cl} above which a part of cloud is converted to precipitation through autoconversion; set equal to $0.5 \cdot 10^{-7} \text{ gm cm}^{-3}$ in the experiment reported in [4]
c_p	specific heat per unit mass at constant pressure ($1.004 \cdot 10^7 \text{ erg gm}^{-1} \text{ deg}^{-1}$)
F	catch coefficient for depletion of cloud by precipitation
e_s	saturation vapor pressure
g	acceleration due to gravity (981 cm sec^{-2})
H	source function for saturation mixing ratio [Eq. (2-22)] and vertical extent of the atmospheric model; set equal to $3 \cdot 10^5 \text{ cm}$
K	parameter in expression for autoconversion of cloud to rain; set equal to 10^{-3} sec^{-1} in the experiment reported in [4]
L	latent heat of evaporation ($2.500 \cdot 10^{10} \text{ erg gm}^{-1}$), and one-half the horizontal extent of the atmospheric model in the x-direction; set equal to $3 \cdot 10^5 \text{ cm}$
n	parameter for size distribution of drops in precipitation; set equal to 10^7 m^{-3}
p	dynamic pressure
P_2	hydrostatic pressure
q	$q_v + q_{cl}$
\bar{q}	$q_{cl} + q_p$

q_{cl}	specific water content in cloud
q_p	specific water content of precipitation
q_s	saturation mixing ratio
q_v	mixing ratio of water vapor
R	gas constant for moist air (287×10^4 erg gm ⁻¹ deg ⁻¹)
R_v	gas constant for water vapor (461.5×10^4 erg gm ⁻¹ deg ⁻¹)
r	relative humidity
S_1, S_2, S_3	source terms for water substance
T	temperature
t	time
u	horizontal component of the wind in the x-direction
V	vertical fall speed of precipitation; set equal to 2×10^4 cm sec ⁻¹ in the experiment reported in [4]
w	vertical component of the wind
x	horizontal coordinate
y	horizontal coordinate
z	vertical coordinate
γ_i	($i = 1, 2, 3, 4$) symbols indicating the presence ($\gamma_i = 1$) or absence ($\gamma_i = 0$) of certain terms
ζ	vorticity for two-dimensional flow
θ	potential temperature
ρ	density
ψ	two-dimensional stream function
\hat{i}	unit vector directed along the positive x-axis
\hat{k}	unit vector directed upward along the vertical
\vec{v}	two-dimensional velocity vector
∇	two-dimensional nabla operator [$\hat{i}(\partial/\partial x) + \hat{k}(\partial/\partial z)$]

APPENDIX B

APPENDIX B




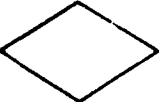




Flow Diagrams

The flow diagrams of the MAIN program and the 16 subroutines of the computer program for the convection simulation model are contained herein. An effort has been made to include a sufficient amount of detail to permit the reader to follow the logical flow of the program.

The symbols used in these diagrams are, for the most part, those which have become standard flow chart symbols. The explanation of the symbols is found in Table 6.

It should be noted that subroutine SUMPk presently applied only to dry convection. This subroutine is being extended to include moist convection.

Table B-1
Flow diagram symbols

Symbol	Meaning
	Direction of flow
	Program step(s)
	Go to subroutine NAME
	Decision based on answer to question posed by contents of the symbol
	Connecting link in flow
	Programmed halt
	Return to calling program at calling point
	Perform the remarks operation by calling subroutine EXCNG

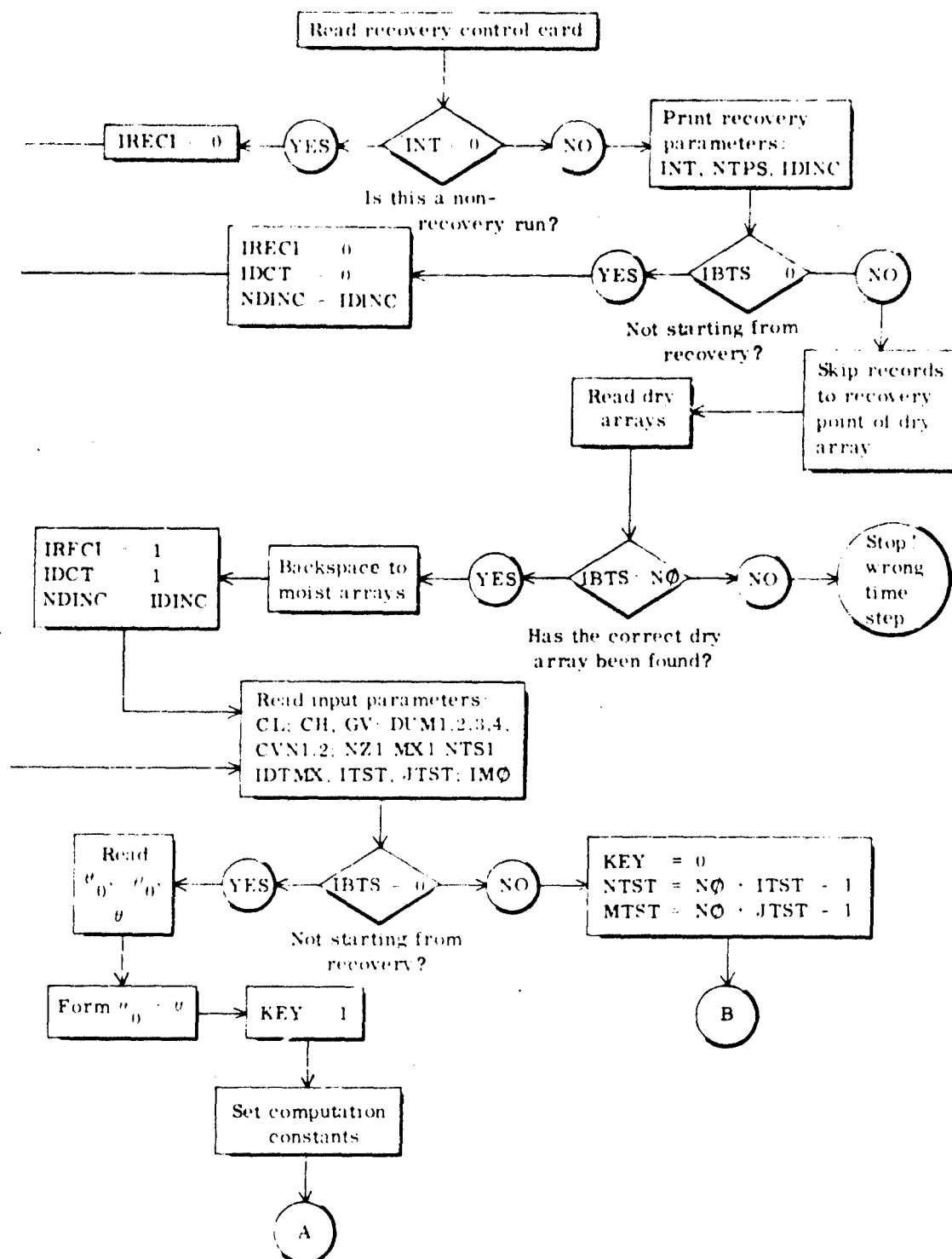


Fig. B-1. MAIN - Directs general flow of computations.

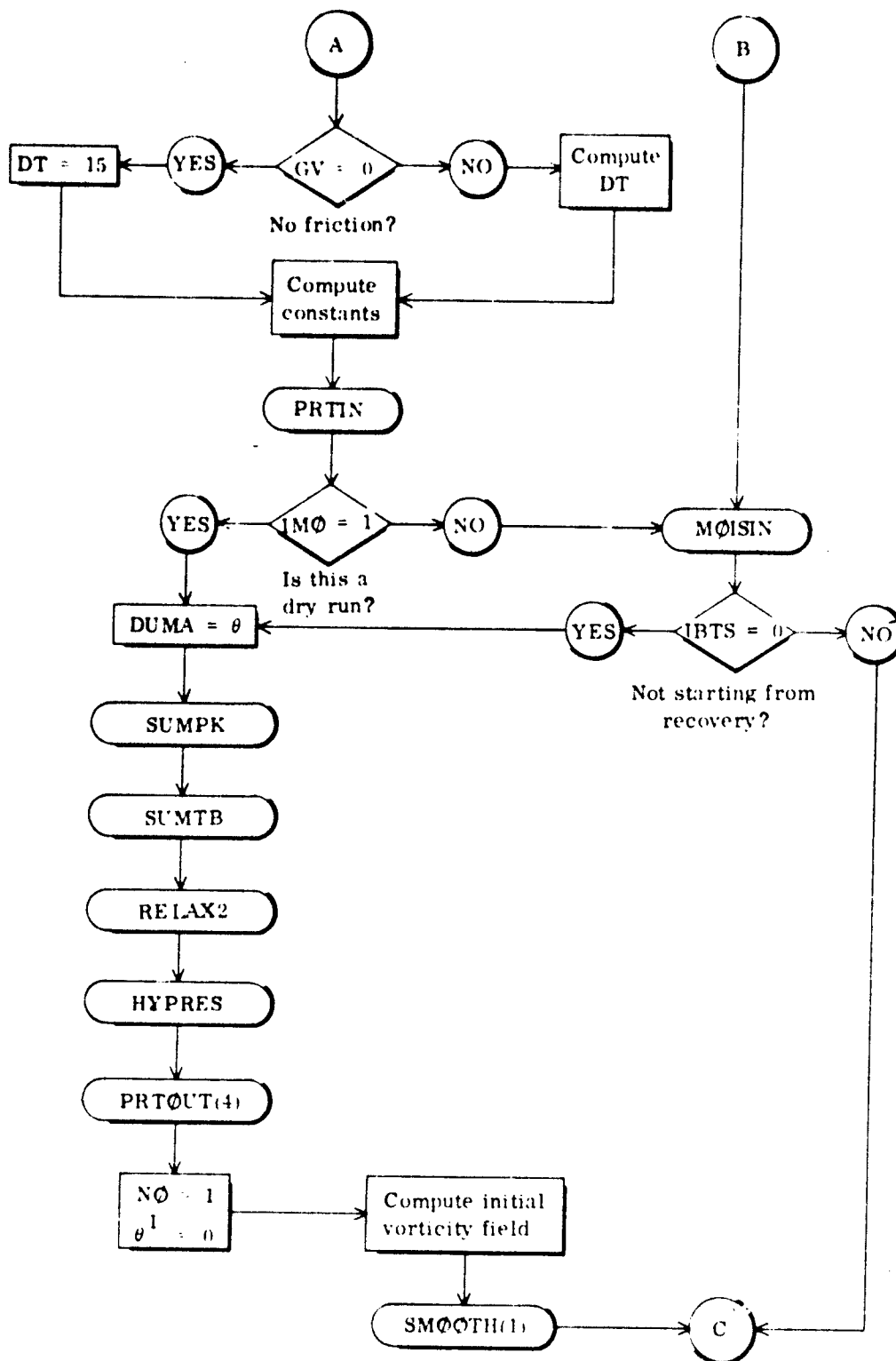


Fig. B-1 (Continued)

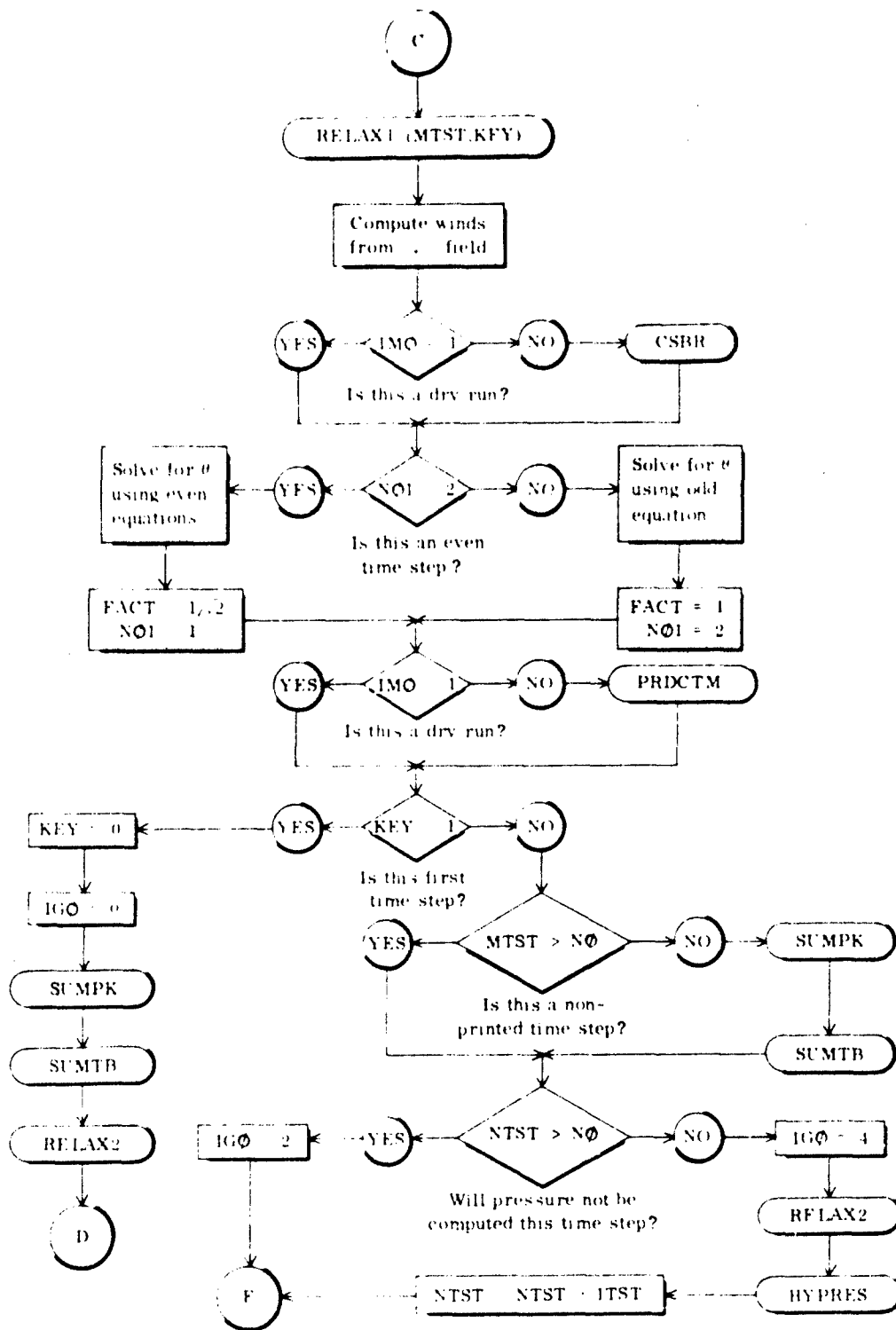


Fig. B-1 (Continued)

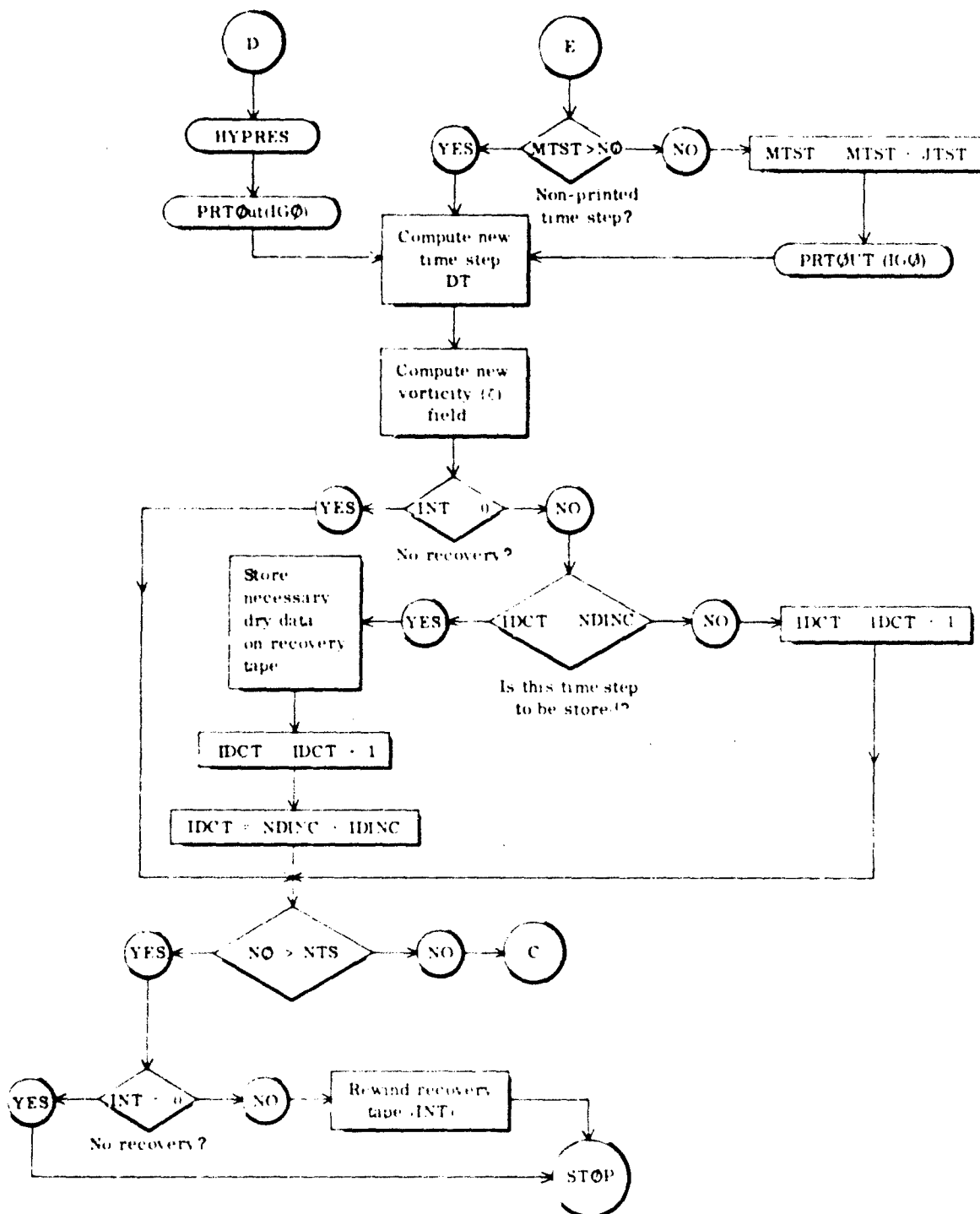


Fig. B-1 (Continued)

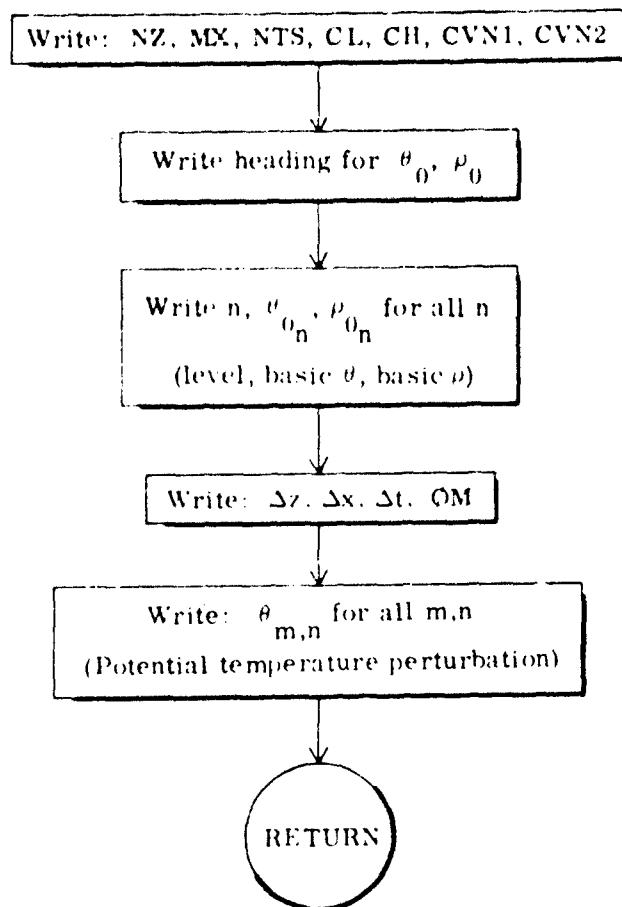


Fig. B-2. PRTIN - Prints "dry" input.

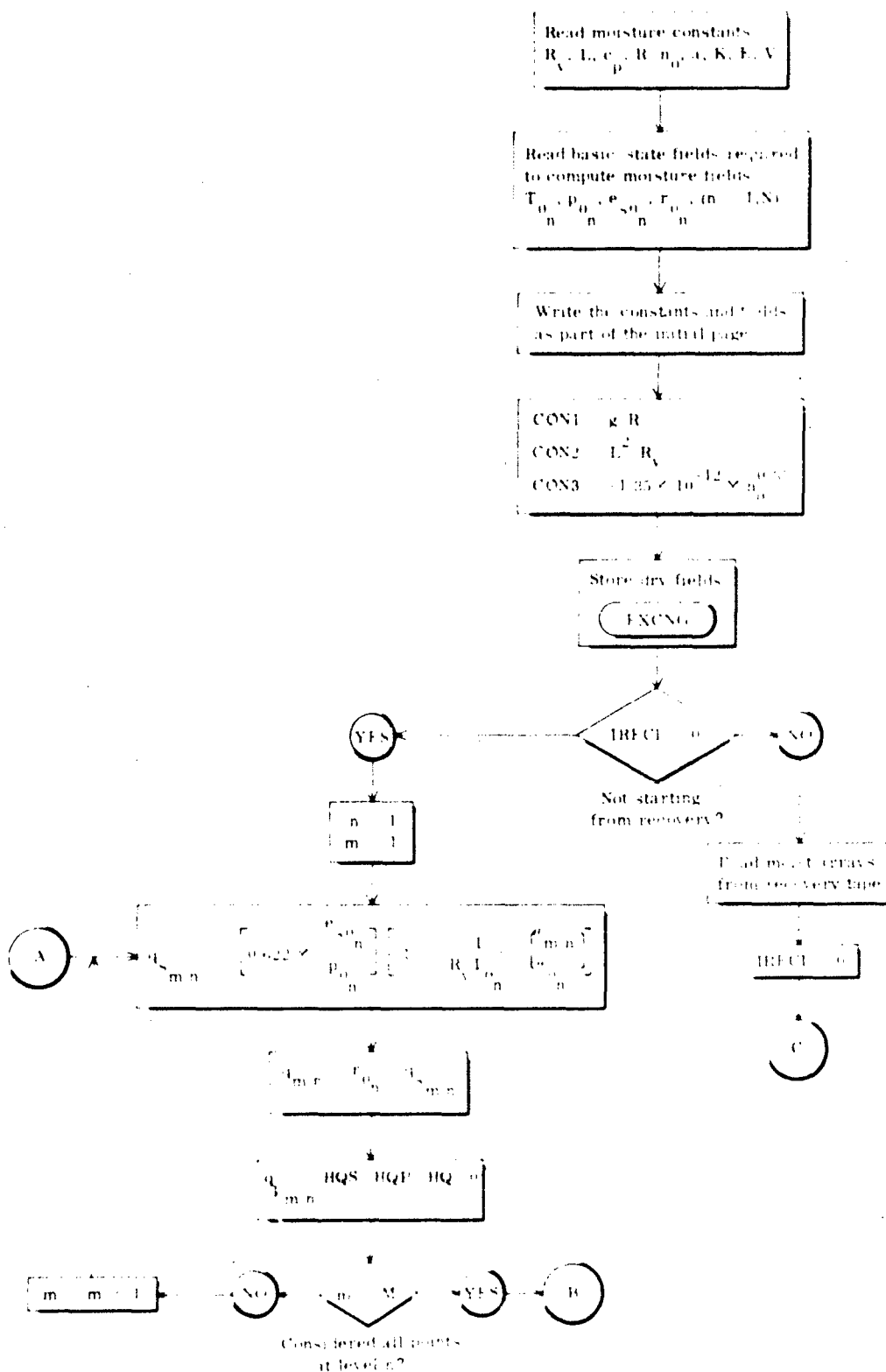


Fig. B-3. MØISIN - Reads and prints "moist" input; computes and prints initial q_s and q fields.

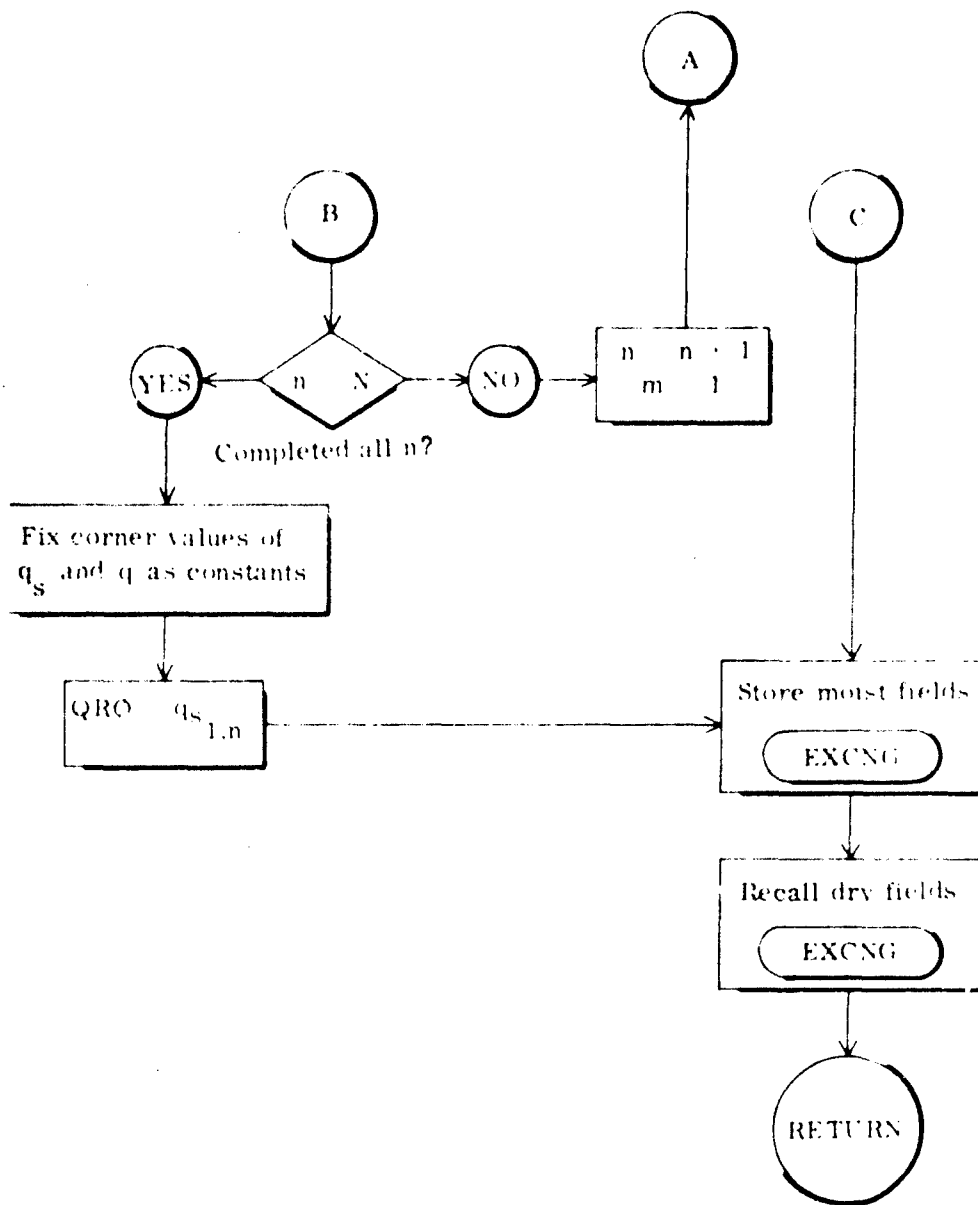


Fig. B-3 (Continued)

NOTE: MTST, KEY, and CVN1 are specified in calling program

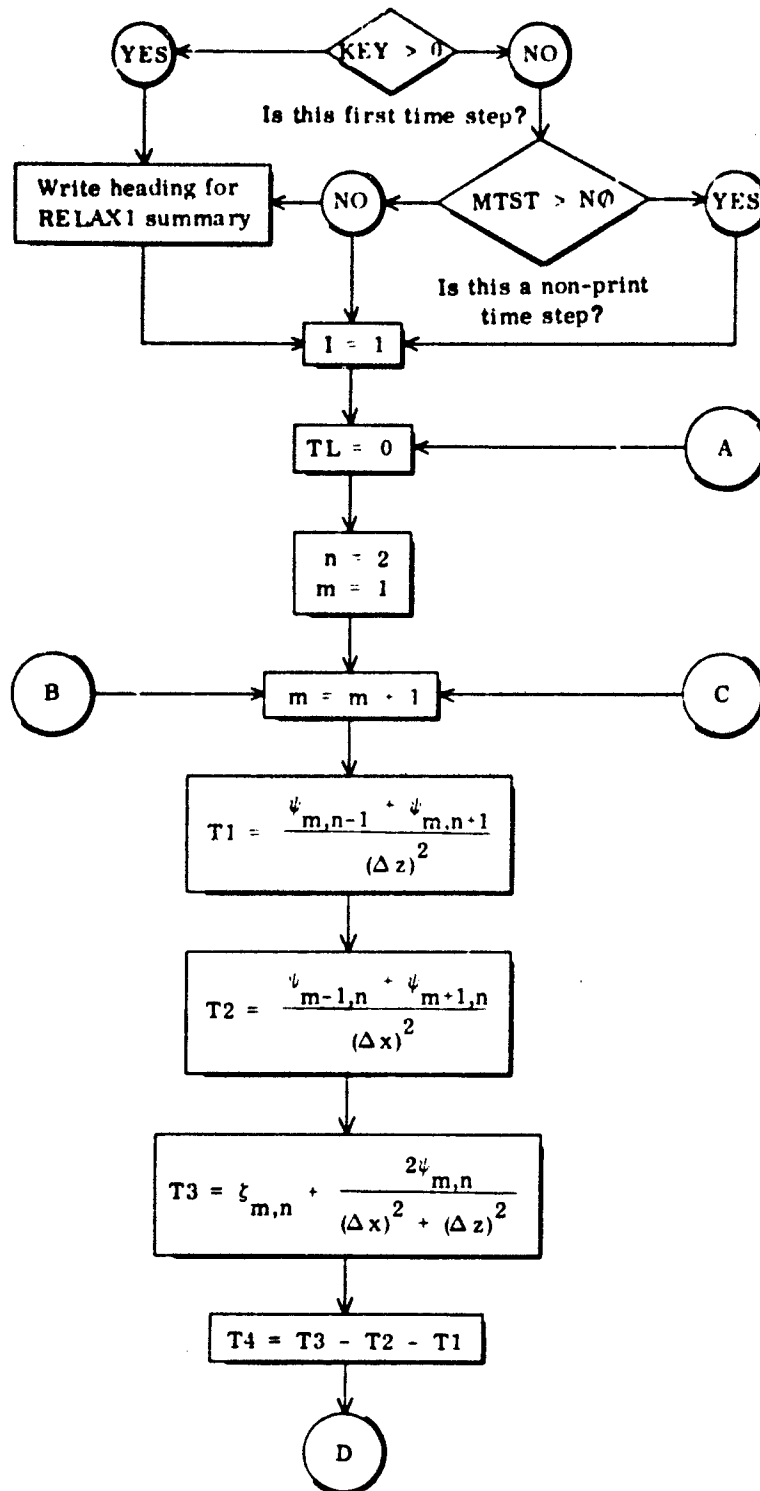


Fig. B-4. RELAX1 - Performs relaxation of ψ -field; prints convergence information.

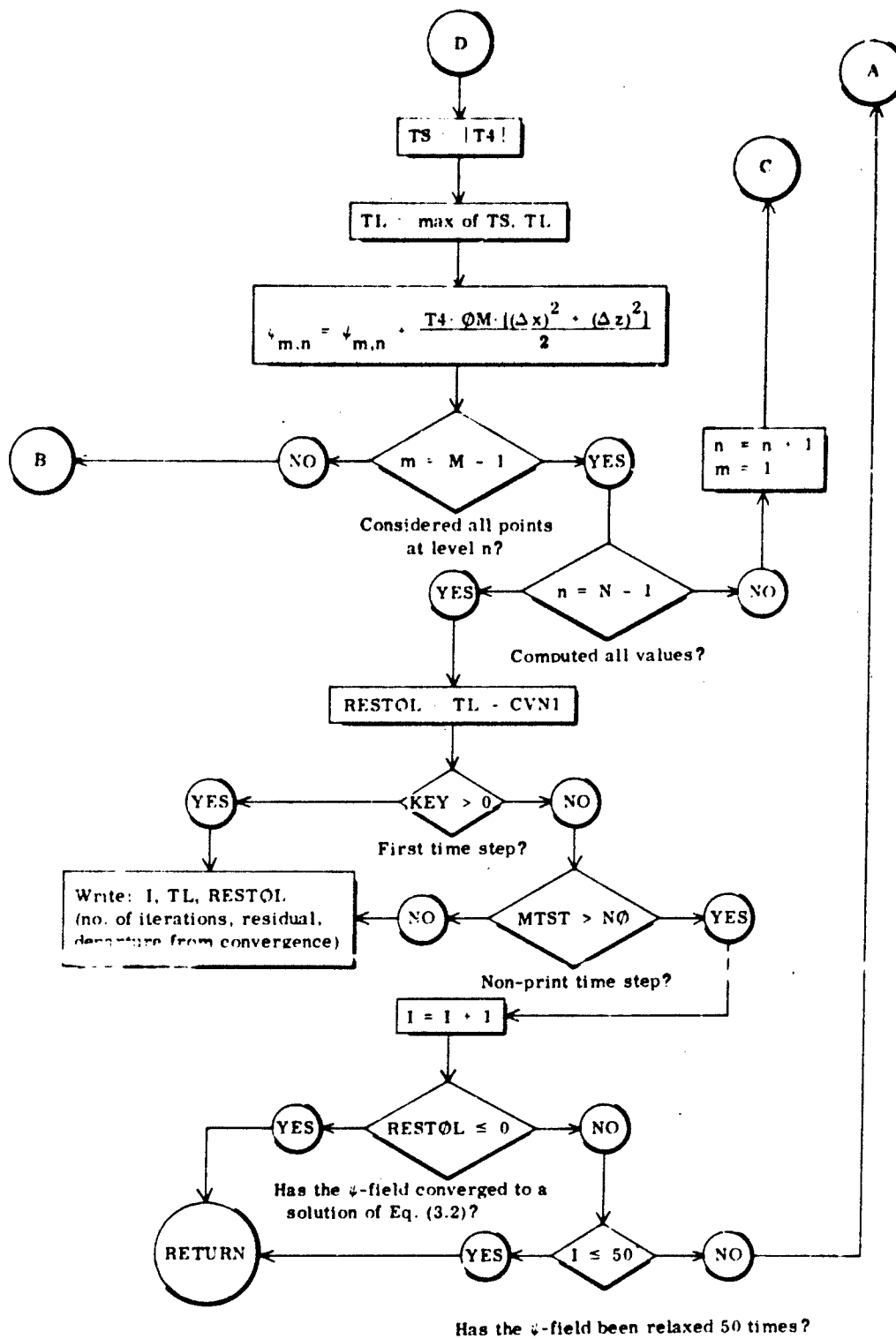


Fig. B-4 (Continued)

NOTE: CVN? specified in calling program

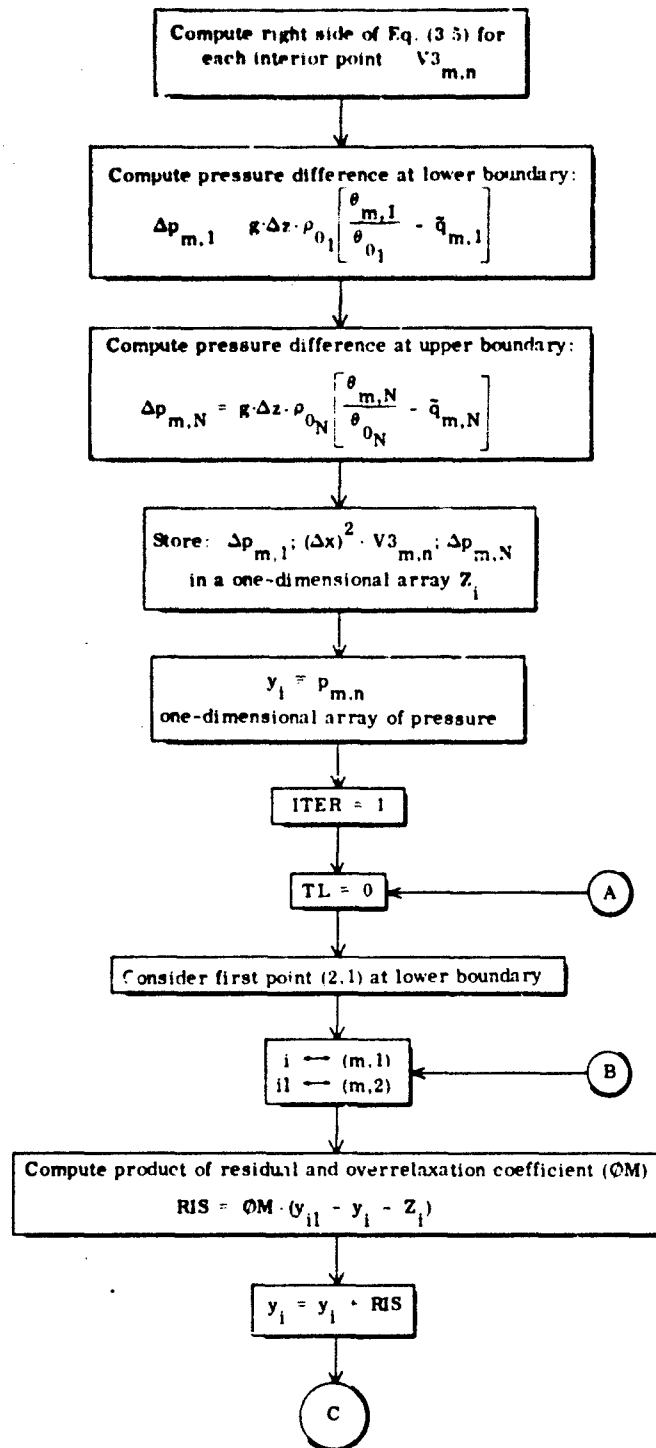


Fig. B-5. RELAX2 - Performs relaxation of p-field; prints convergence information.

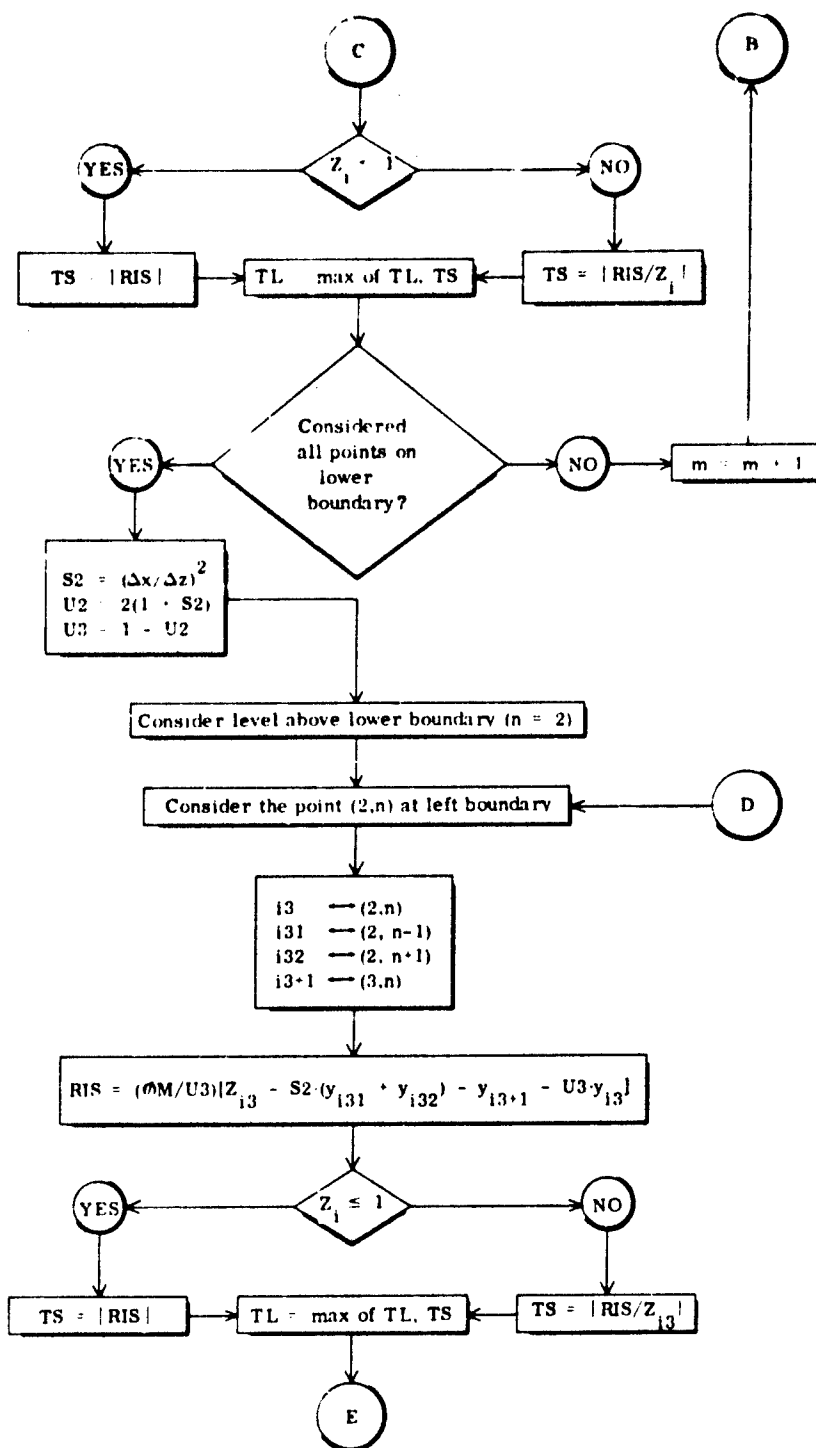


Fig. B-5 (Continued)

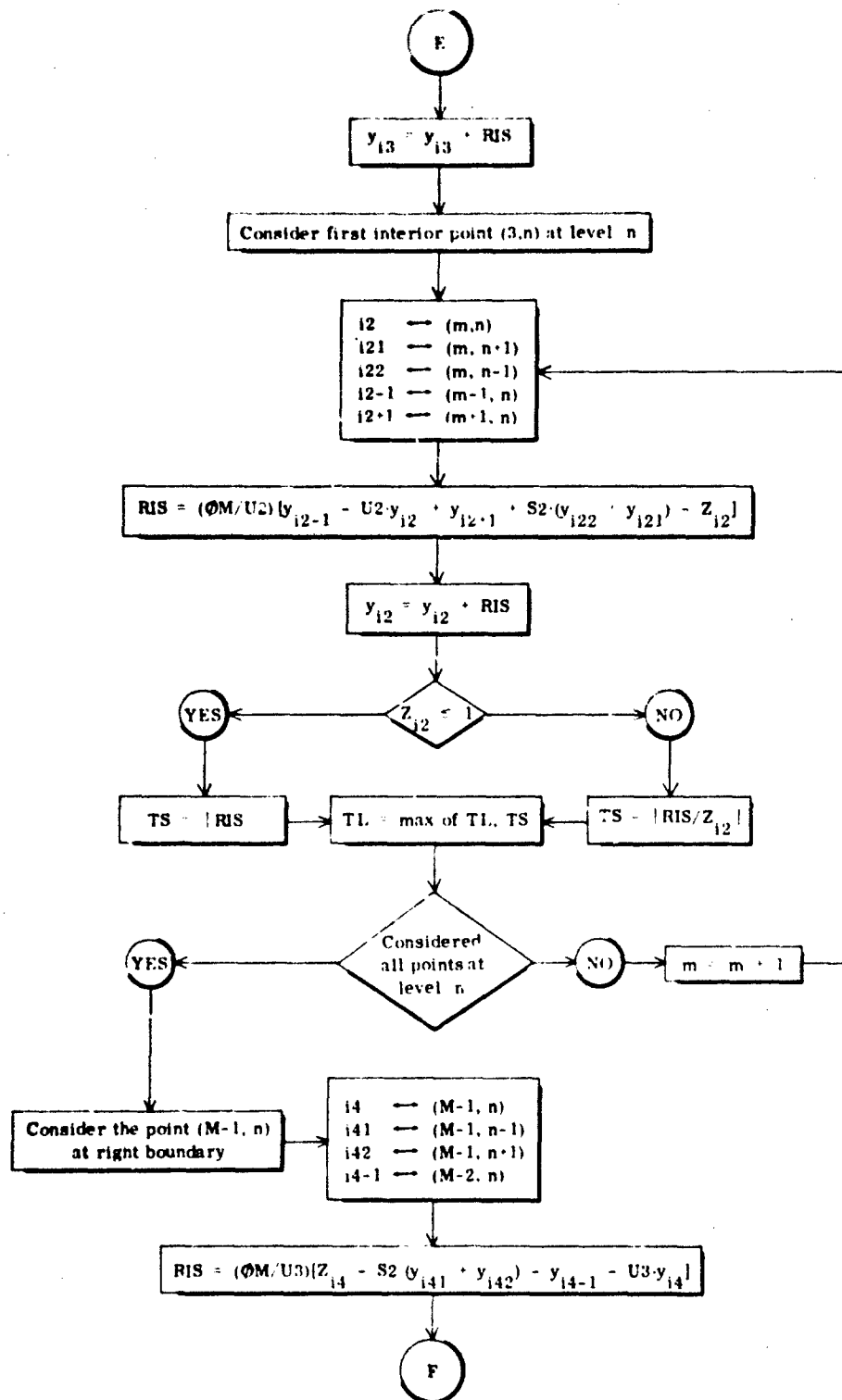


Fig. B-5 (Continued)

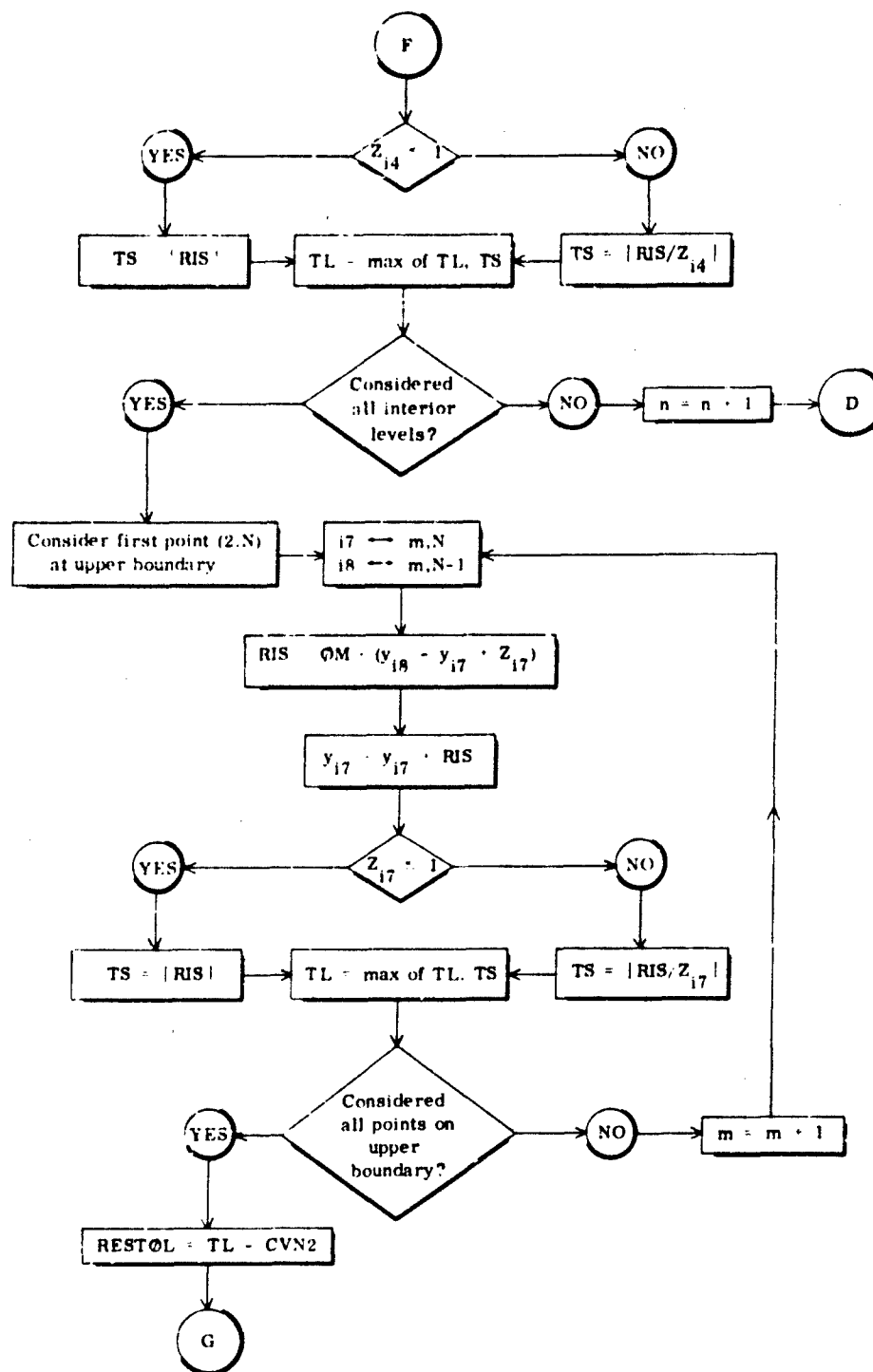


Fig. B-5 (Continued)

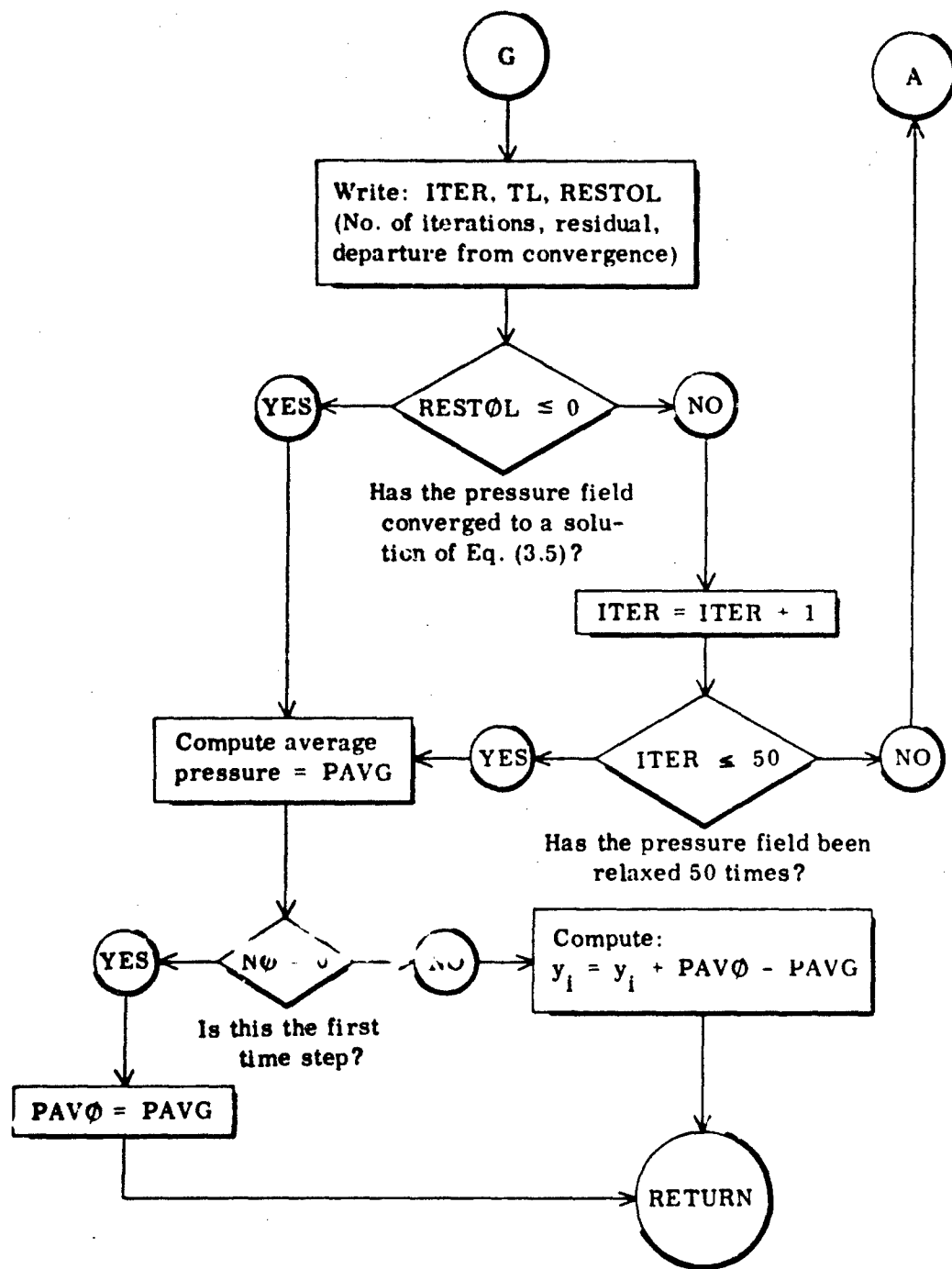


Fig. B-5 (Continued)



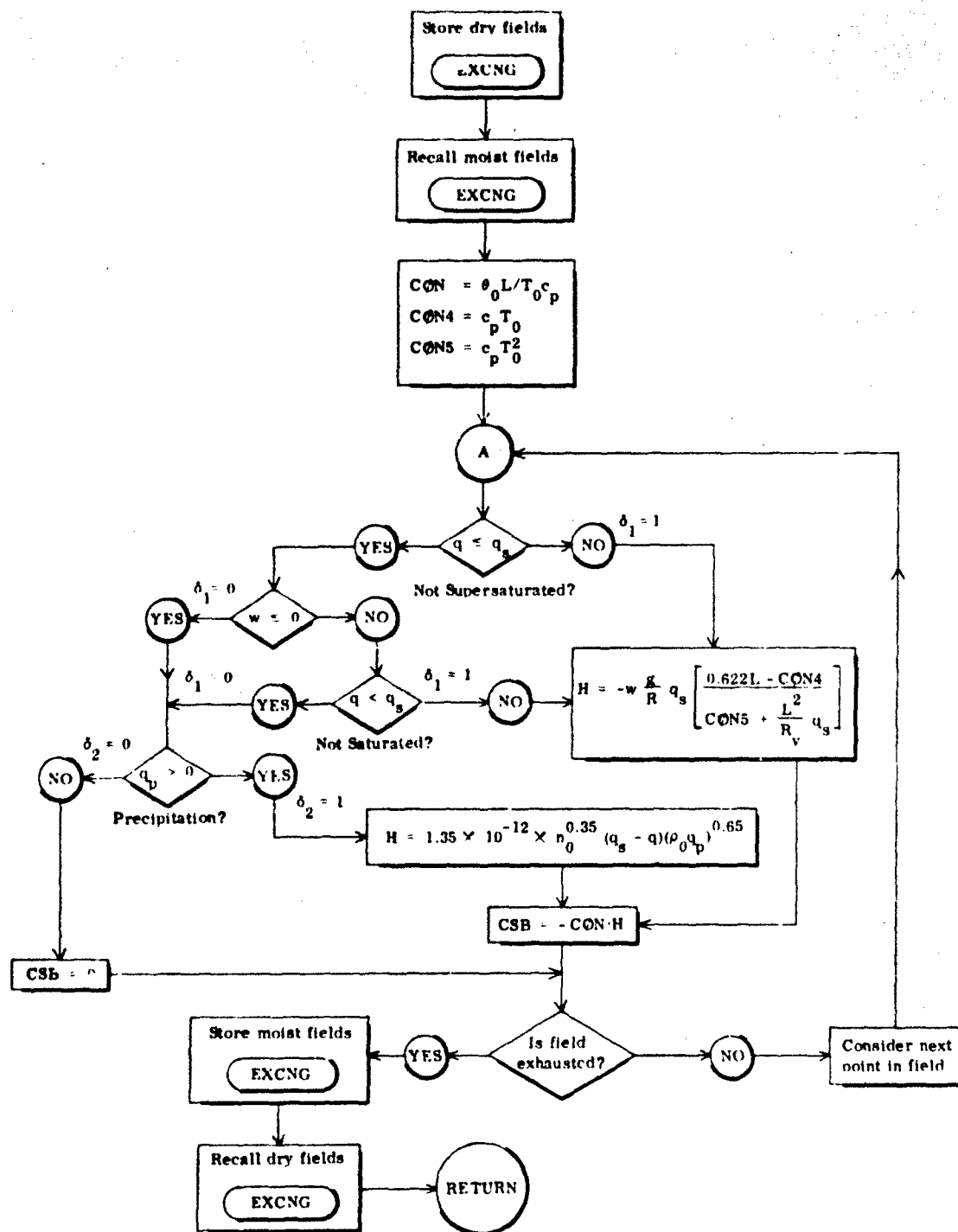


Fig. B-7. CSBR - Computes source function for θ -prediction.

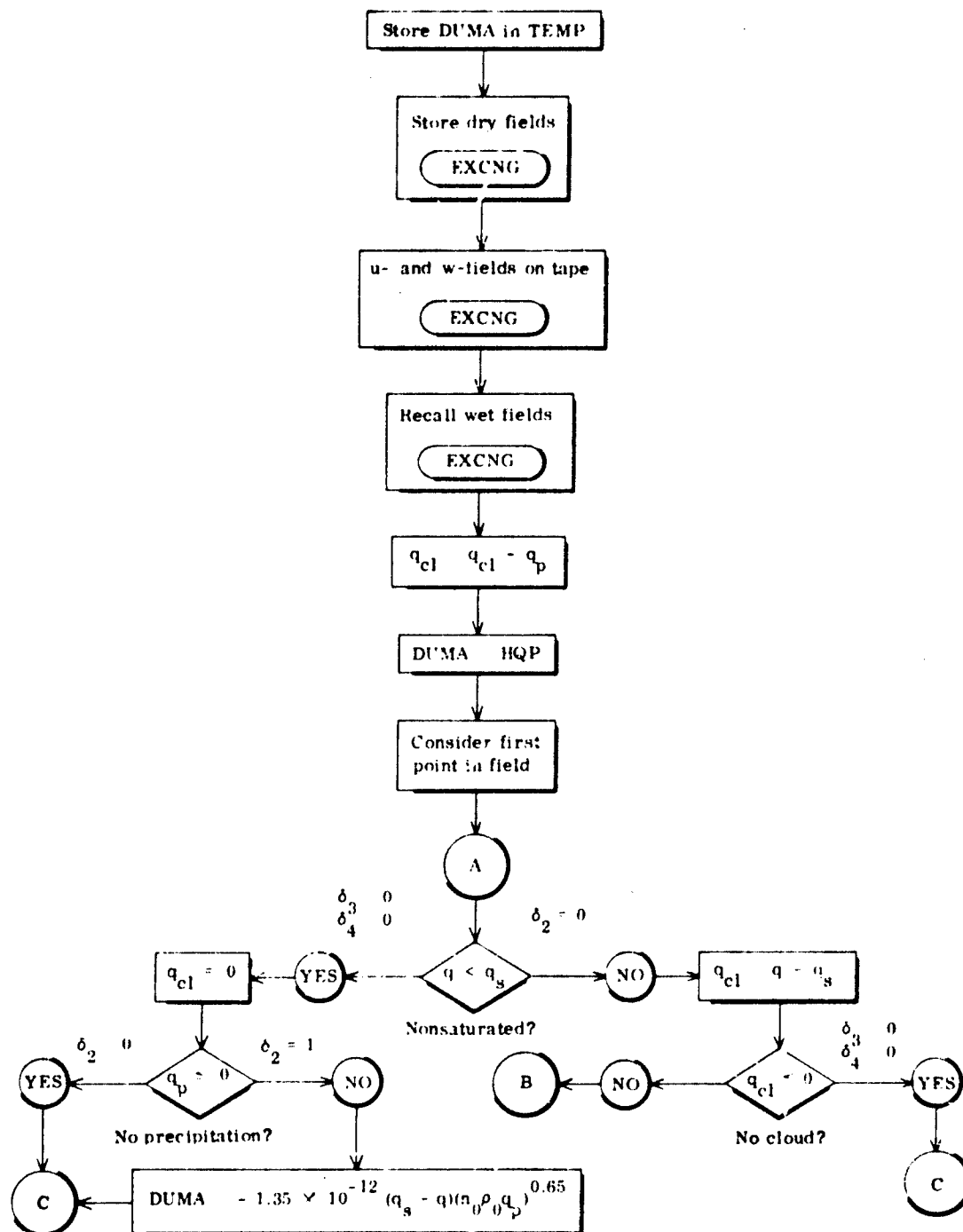


Fig. B-8. PRDCTM - Computes source function for, and controls prediction of q_n , q_w , and q .

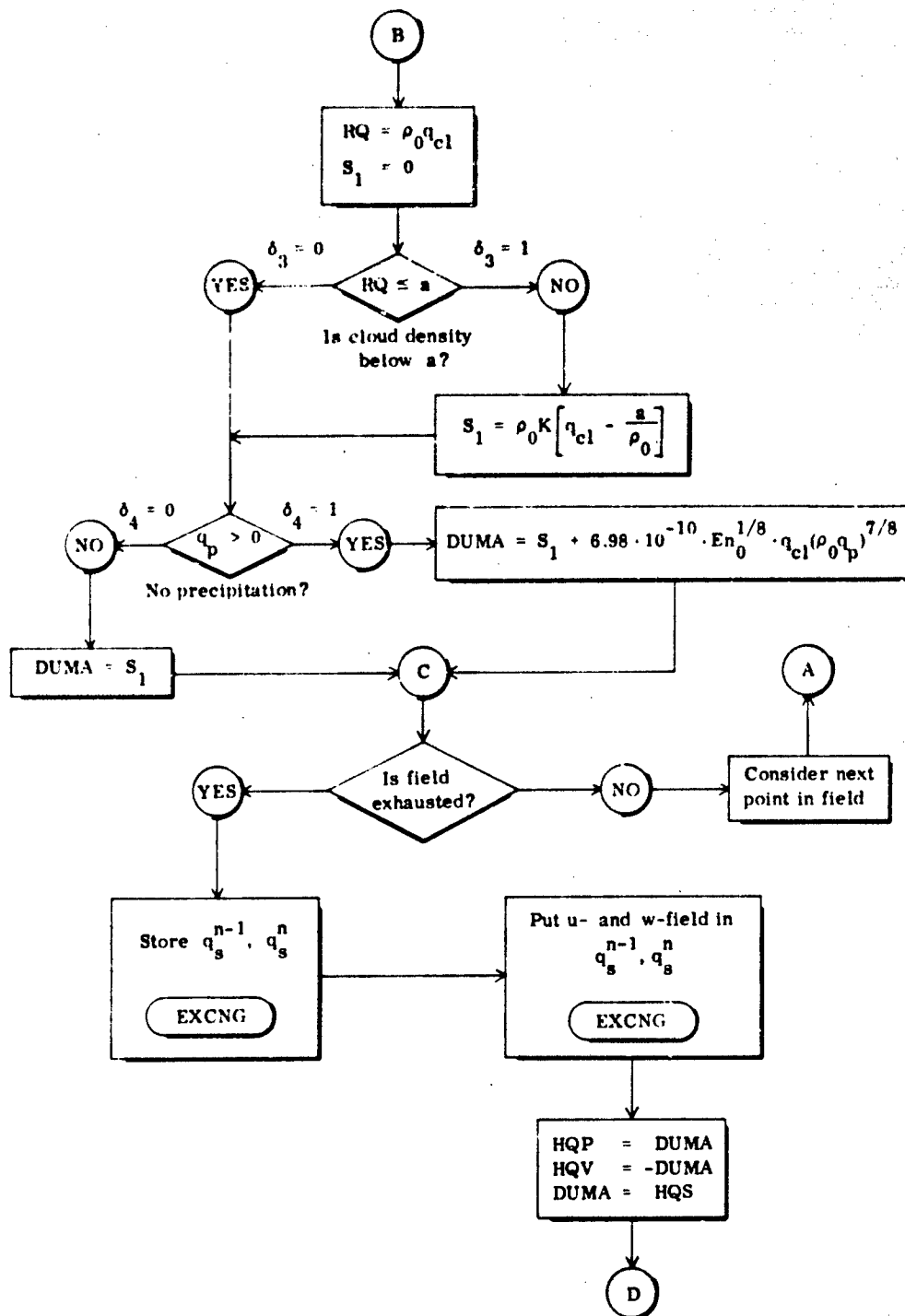


Fig. B-8 (Continued)

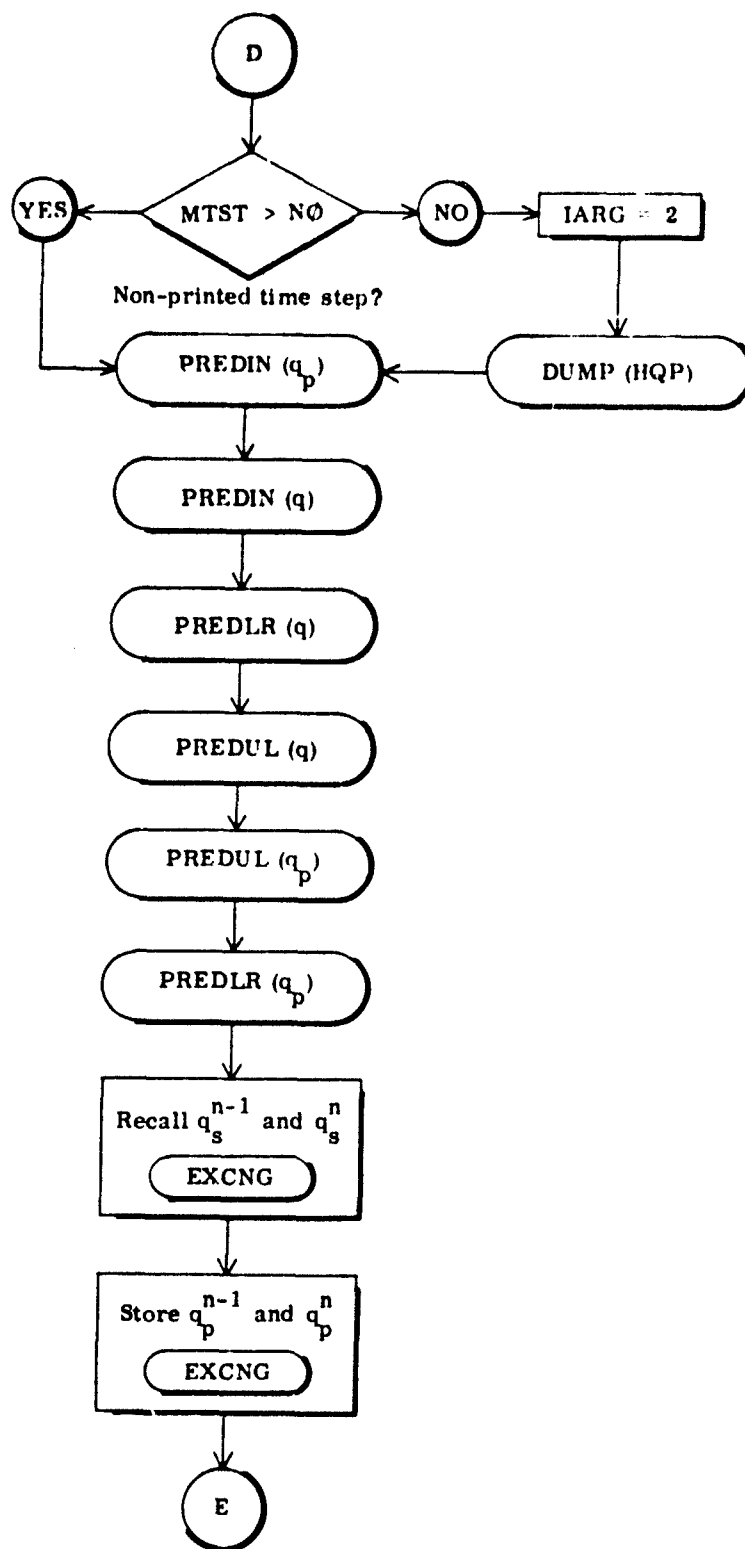


Fig. B-8 (Continued)

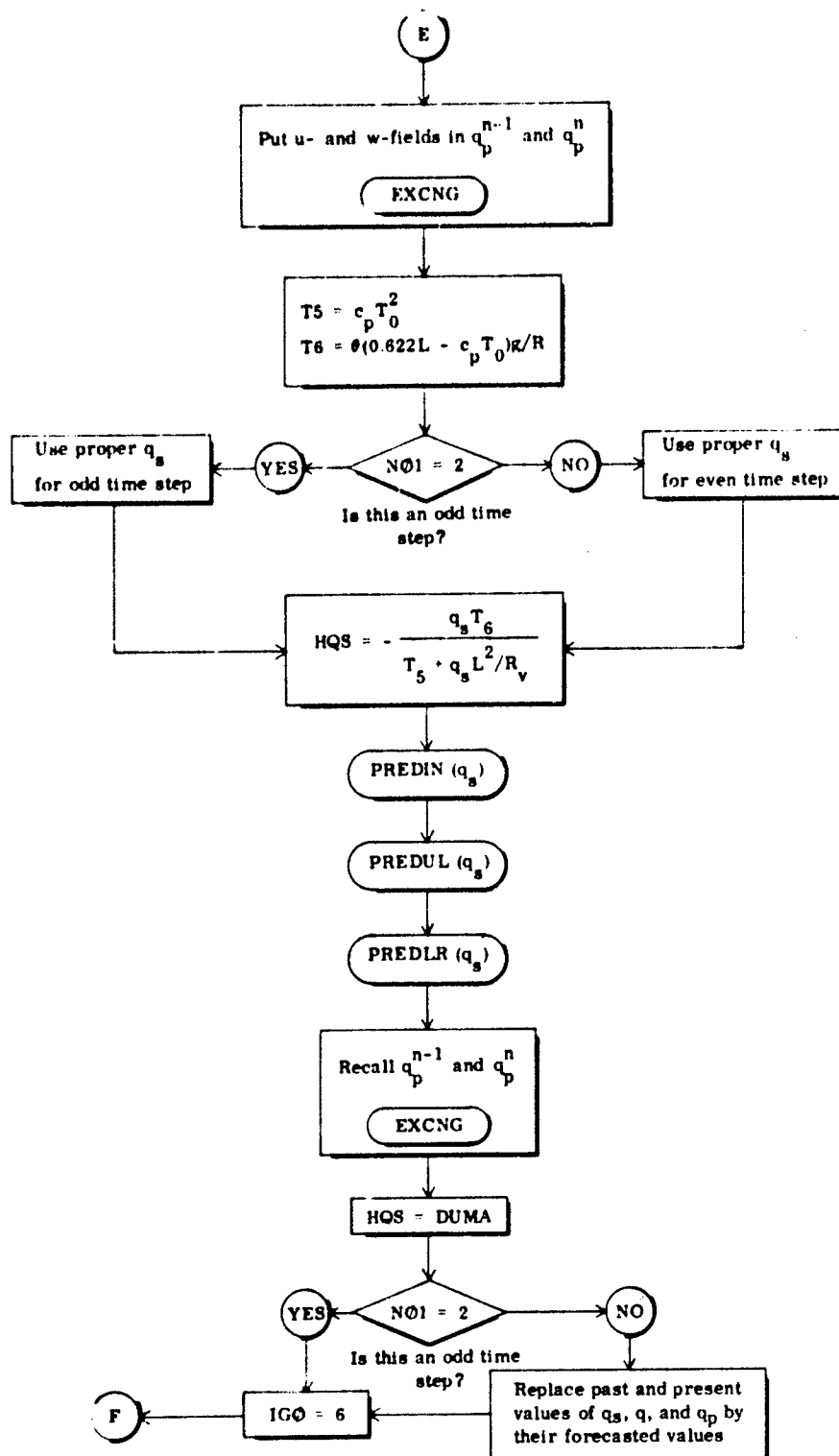


Fig. B-8 (Continued)

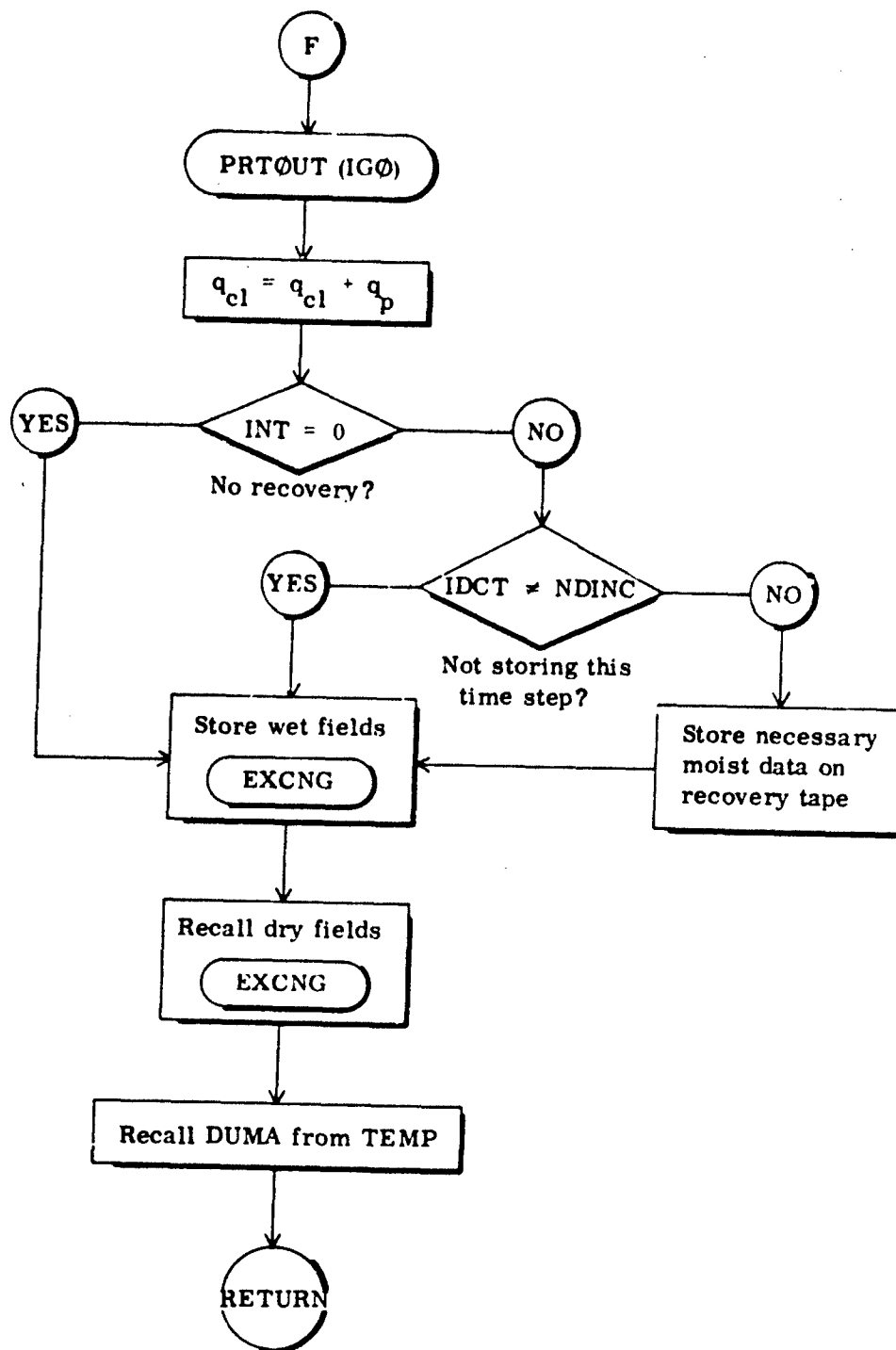


Fig. B-8 (Continued)

- NOTE: 1. $QR(QR\phi)$ is a dummy variable for $q(q_0)$, $q(q_{s0})$, or q_p
 2. IADT is specified by calling program to modify the routine for q_p

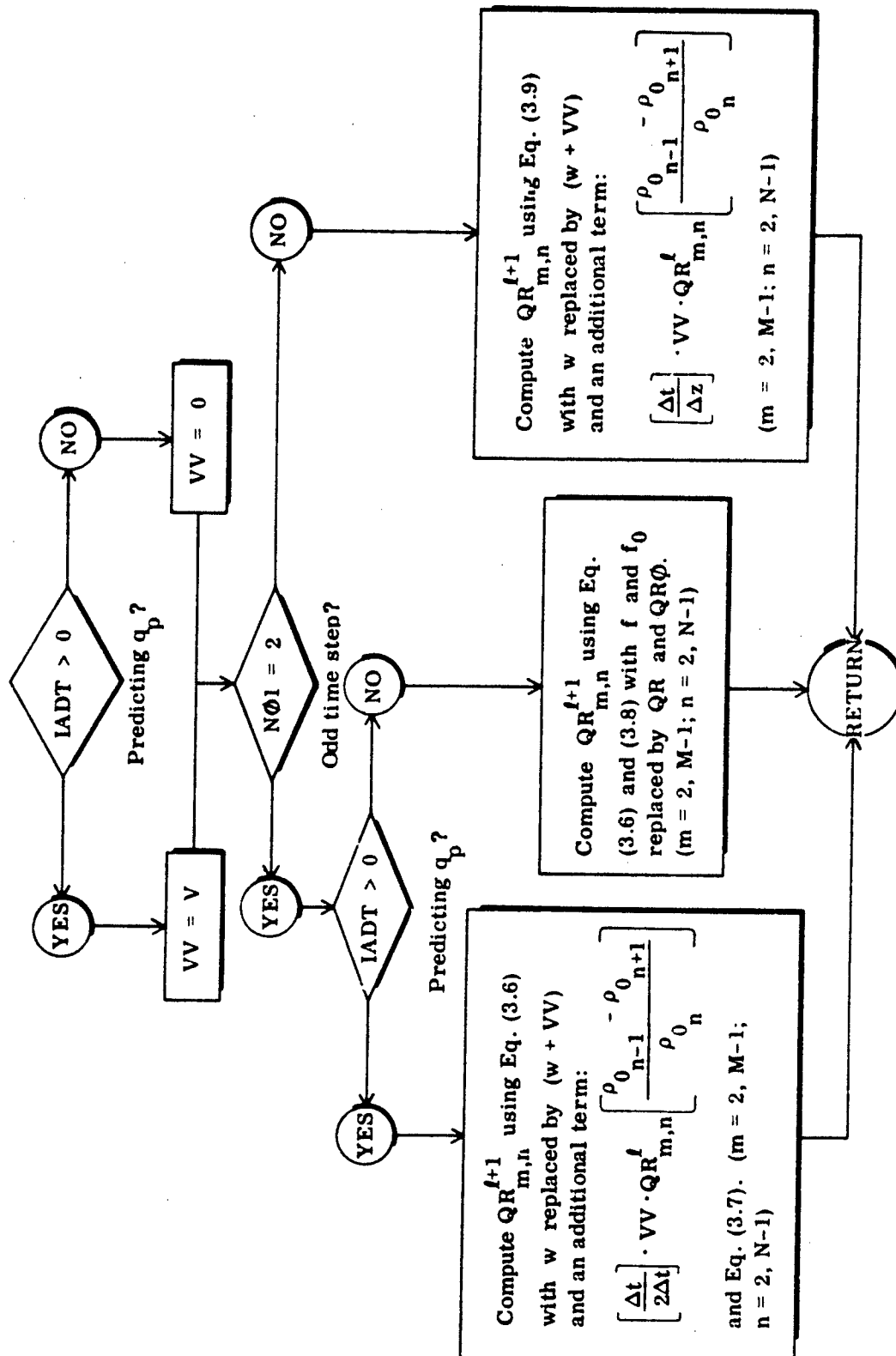


Fig. B-9. PREDIN - Predicts values of q_p , q_s , and q for interior points.

- NOTE: 1. QR is a dummy argument for q , q_s , or q_p
 2. IADT is specified by calling program to control special routine for q_p

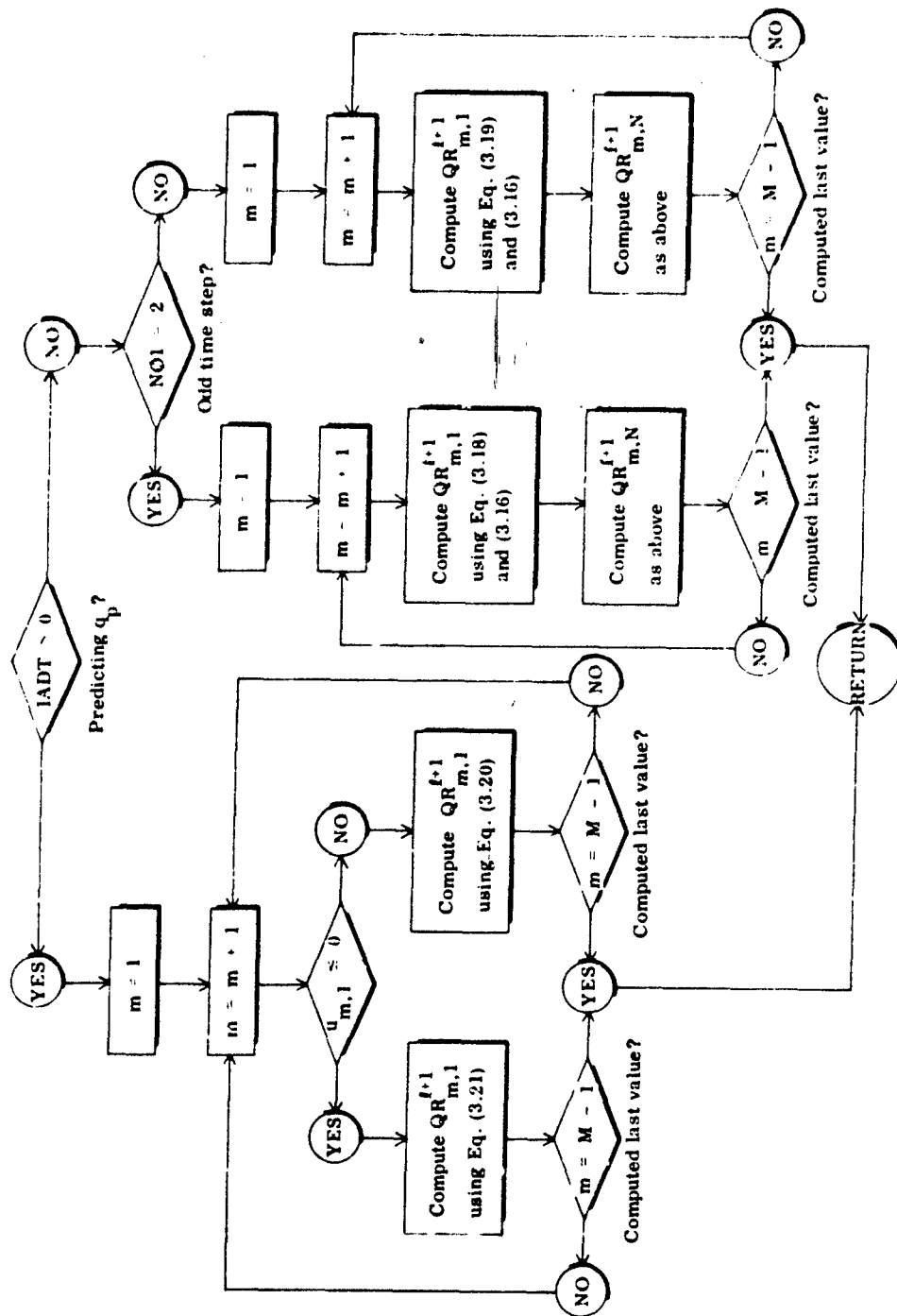


Fig. B-10. PREDUL - Predicts upper and lower boundary values of q_p , q_s , and q .

NOTE: 1. $QR(QRQ)$ is a dummy argument for $q(q_0)$, $q_s(q_{s0})$, or q_p .

2. LADT is specified by calling program to control special routine for q_p .

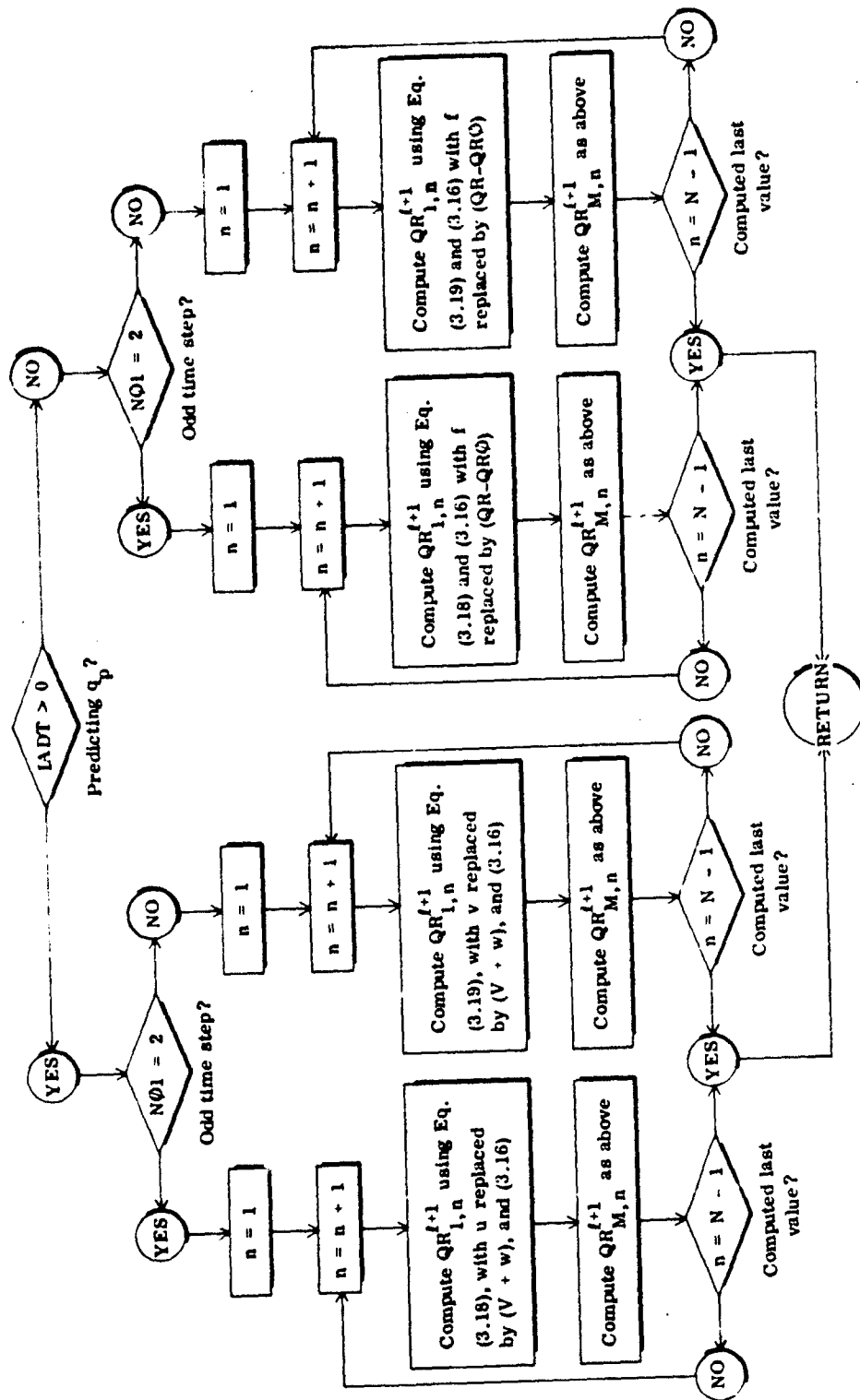


Fig. B-11. PREDLR - Predicts lateral boundary values of q_p , q_s , and q .

(MM, NN, IWAY, and NTAPE are specified in calling program)

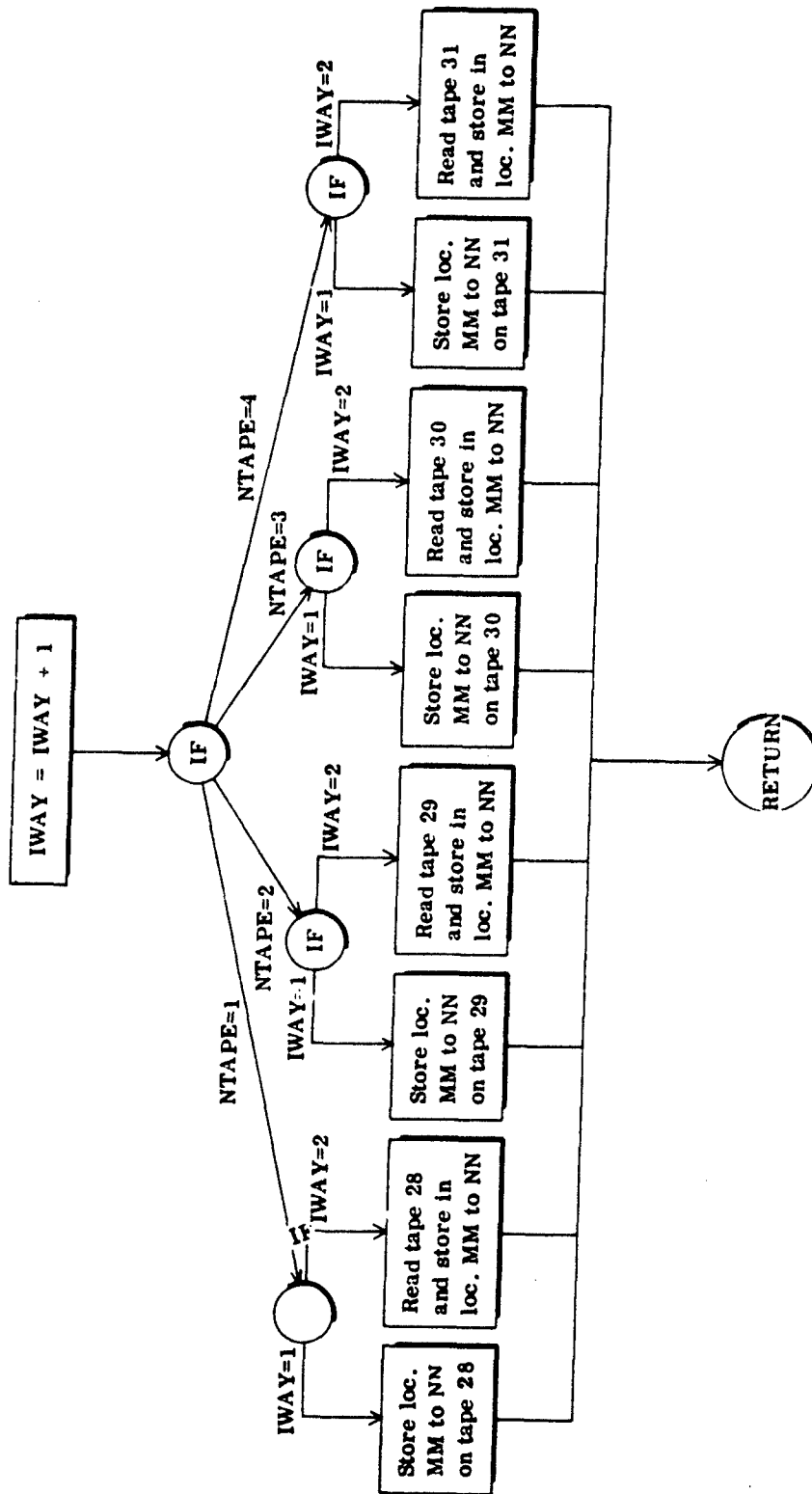


Fig. B-12. EXCNG - Selectively controls flow of arrays to and from auxiliary storage.

NOTE: MKEY is specified in calling program

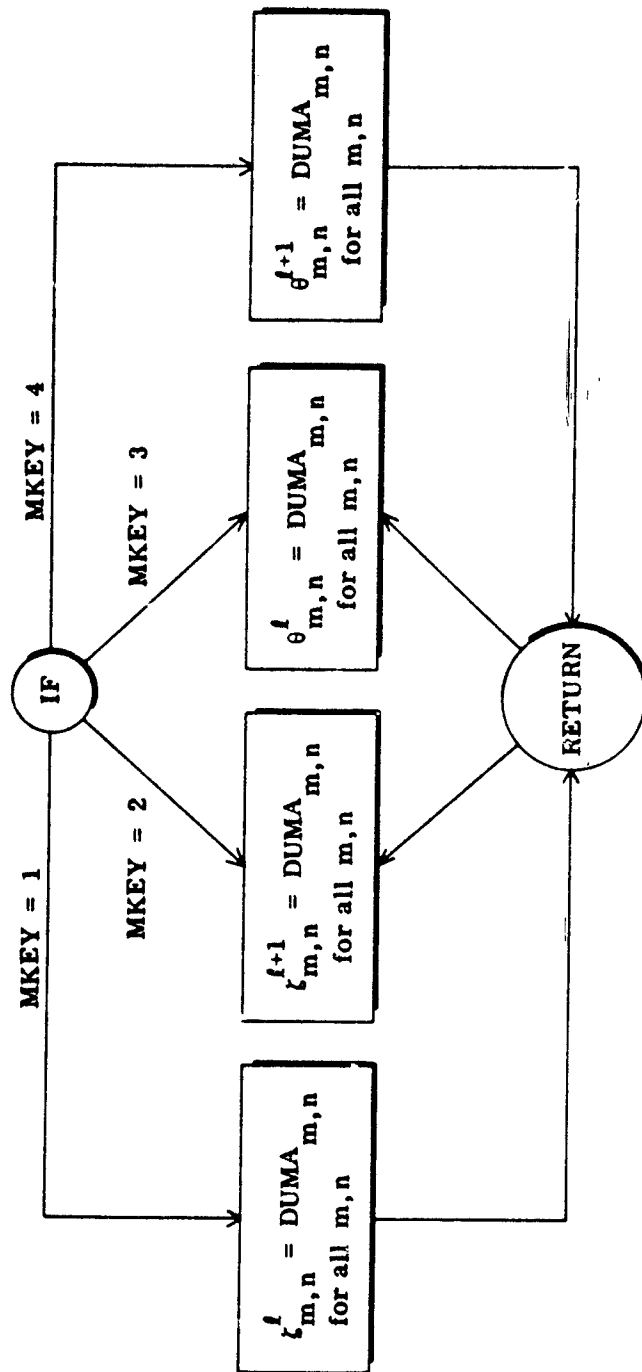


Fig. B-13. SMOOTH - Transfers fields from dummy array (DUMA) to proper array.

- NOTE: 1. ARG is a dummy argument for CSB or HQP as specified in calling program.
2. LARG is specified in calling program.

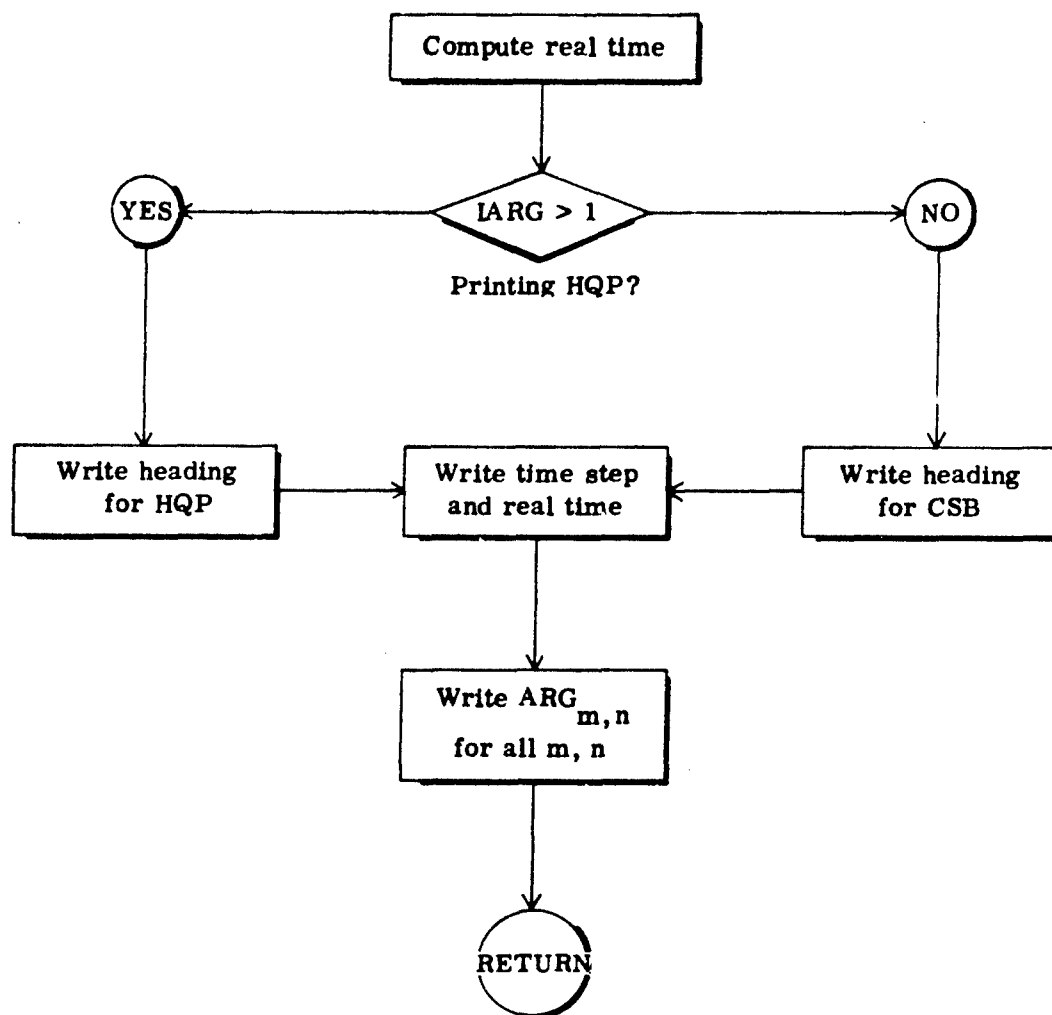


Fig. B-14. DUMP - Prints source functions for θ and q_p .

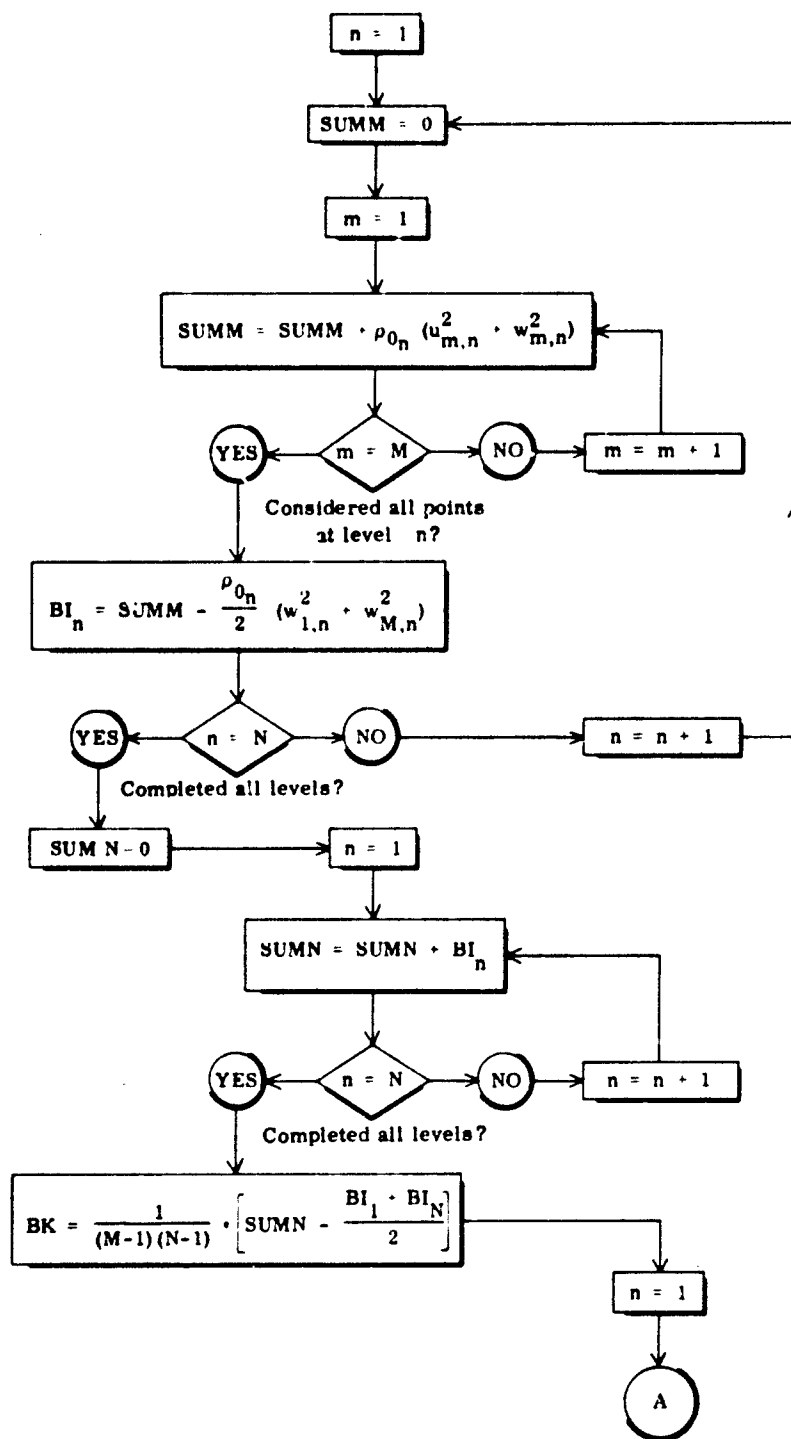


Fig. B-15. SUMPK - Computes and prints space averaged potential and kinetic energies and their difference.

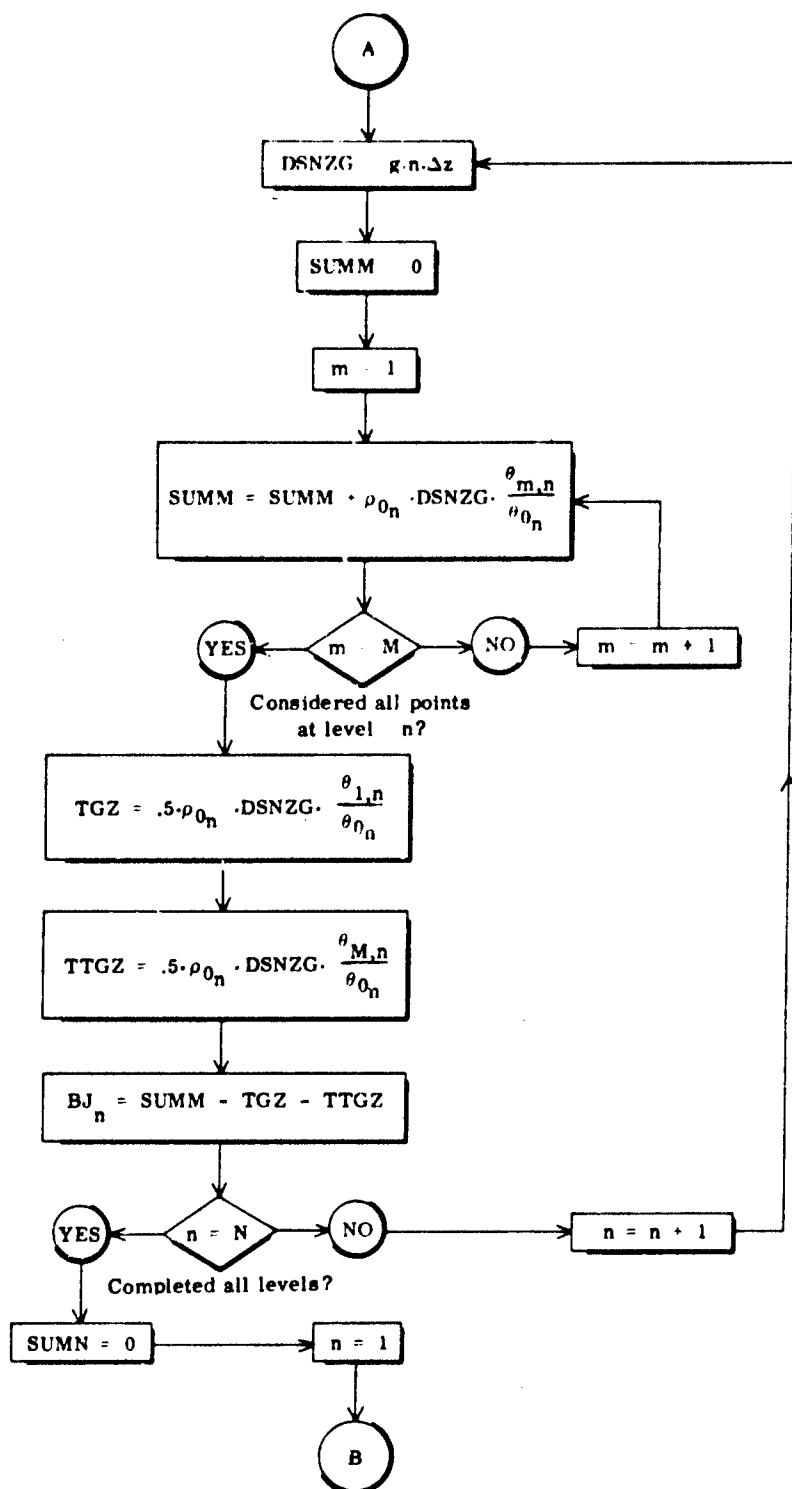


Fig. B-15 (Continued)

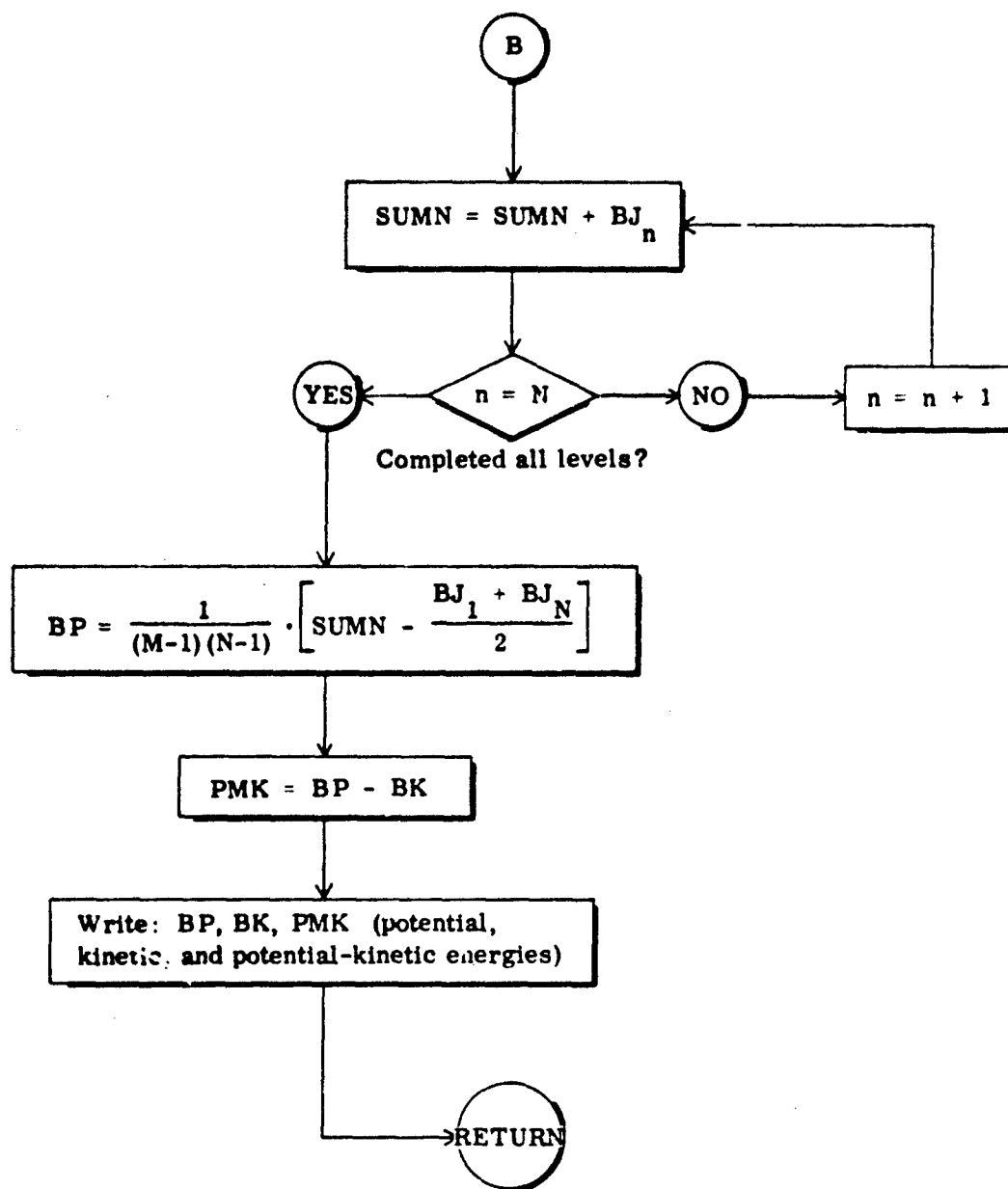


Fig. B-15 (Continued)

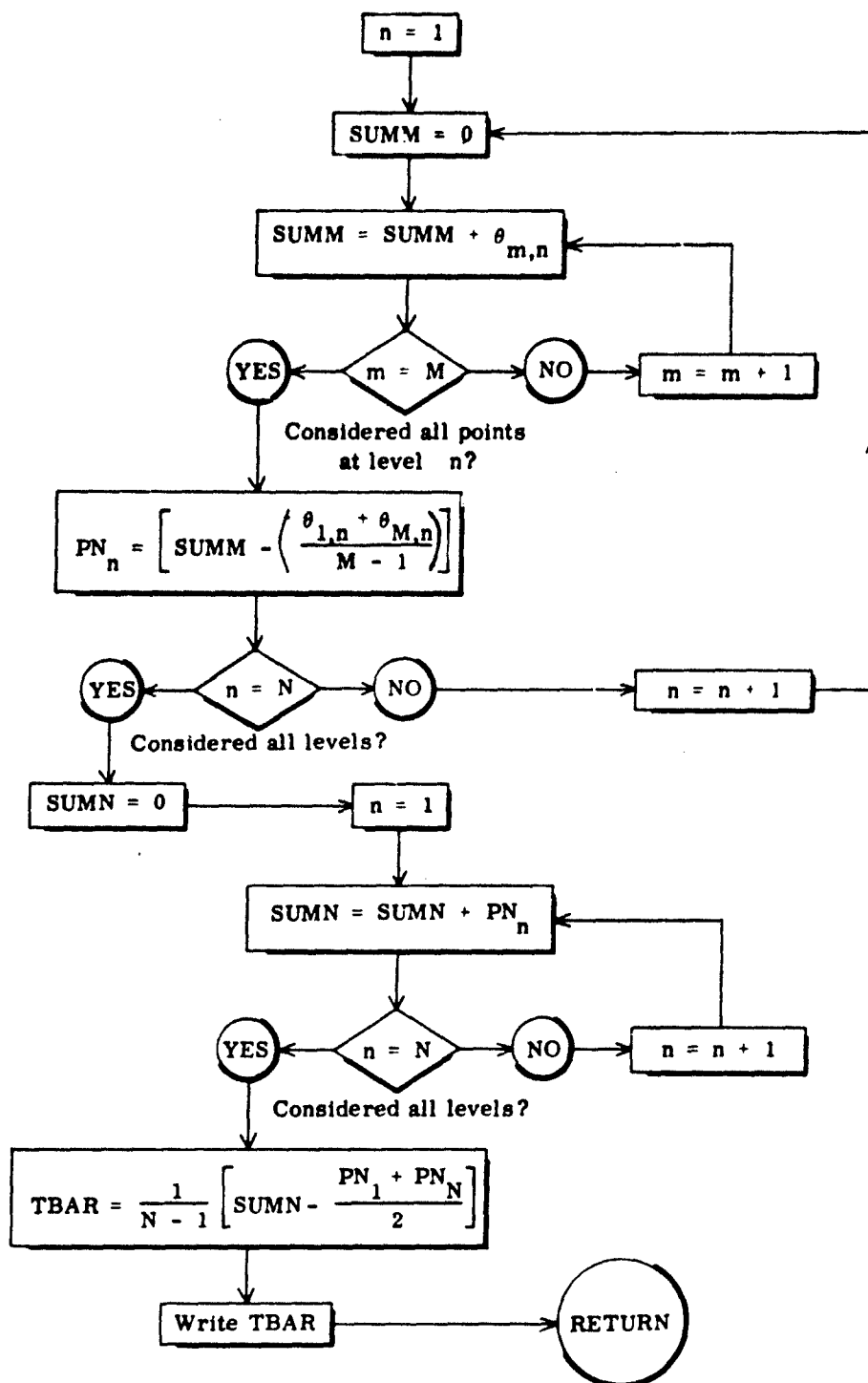


Fig. B-16. SUMTB - Computes and prints space averaged potential temperature.

(IGQ - Specified in Calling Program)

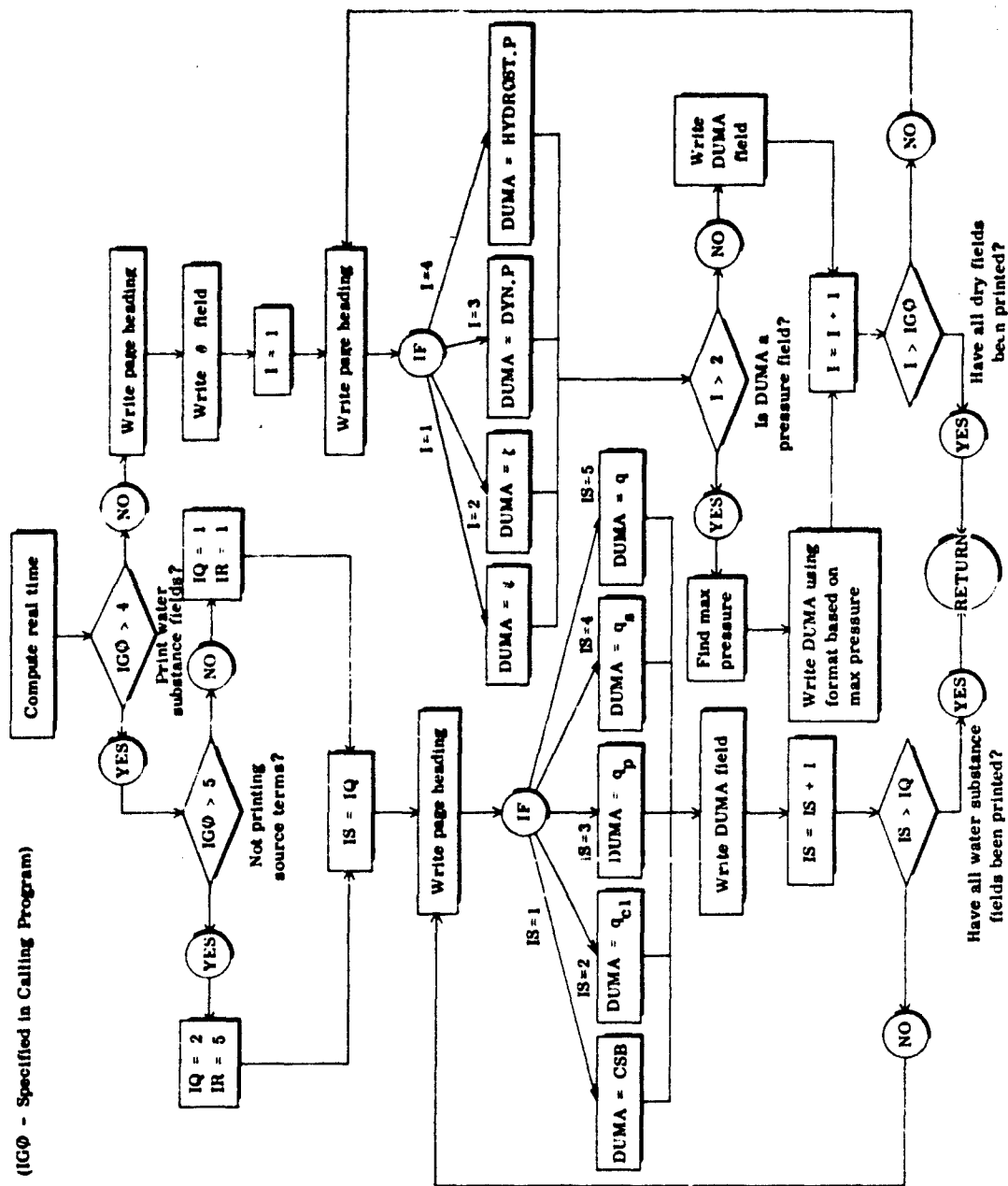


Fig. B-17. PRINTOUT - Prints the θ , ψ , ζ , p , $P2$, q_{c1} , q_p , q_s , and q fields.

Security Classification

DOCUMENT CONTROL DATA - R & D

(Security classification of title, body of abstract and indexing annotation must be entered when the overall report is classified)

1. ORIGINATING ACTIVITY (Corporate author) The Travelers Research Center, Inc. 250 Constitution Plaza Hartford, Connecticut 06103		2a. REPORT SECURITY CLASSIFICATION Unclassified	
		2b. GROUP N/A	
3. REPORT TITLE Relationships Between Tropical Precipitation and Kinematic Cloud Models			
4. DESCRIPTIVE NOTES (Type of report and inclusive dates) Annual Report No. 1, 1 Nov 66 - 30 Apr 67			
5. AUTHOR(S) (First name, middle initial, last name) G. Arnason and R. S. Greenfield			
6. REPORT DATE June 1967		7a. TOTAL NO. OF PAGES 80	7b. NO. OF REFS 4
8a. CONTRACT OR GRANT NO. DA28-043 AMC-02192(E)		8b. ORIGINATOR'S REPORT NUMBER(S) 7482-257	
a. PROJECT NO.		8c. OTHER REPORT NO(S) (Any other numbers that may be assigned this report) ECOM 02192-2	
10. DISTRIBUTION STATEMENT Distribution of this document is unlimited.			
11. SUPPLEMENTARY NOTES None.		12. SPONSORING MILITARY ACTIVITY US Army Electronics Command AMSEL-BL-AP Fort Monmouth, New Jersey 07703	
13. ABSTRACT <p>The mathematical formulation and associated finite-difference approximations for the numerical model of a precipitating roll cloud are summarized. With that background, the computer program used to perform the computations in experiments simulating moist convection is described in detail.</p> <p>The program description includes discussion of the input requirements, the internal operations, and the output. The newly developed recovery feature of the program is explained. All options, presently available in the program, are described. The detailed description of the computer program is contained in individual flow diagrams of the main program and the 16 subroutines.</p> <p>In the concluding remarks, the present status of the computer program is given. Finally, the anticipated future plans for the program are outlined.</p>			

DD FORM 1473

REPLACES DD FORM 1473, 1 JAN 64, WHICH IS OBSOLETE FOR ARMY USE.

Security Classification

Security Classification

14. KEY WORDS	LINK A		LINK B		LINK C	
	ROLE	WT	ROLE	WT	ROLE	WT
Thermal convection Buoyant bubble Toroidal circulation Numerical experiments Non-hydrostatic pressure						

Security Classification